UNIVERSITY OF CALIFORNIA SAN DIEGO

On the Lateral Habenula: Neurotransmitter Co-Release and a Neural Circuit Controlling Discouragement

A dissertation submitted in partial satisfaction
of the requirements for the Doctor of Philosophy

in

Neurosciences

by

Sage Ryan Aronson

Committee in charge:

Professor Roberto Malinow, Chair
Professor Christina Gremel
Professor Jeffry Isaacson
Professor Takaki Komiyama
Professor Nicholas Spitzer

2019

The dissertation of Sage Ryan Aronson is approved, and it is acceptable in quality and form for publication on microfilm and electronically:

_____

_____

_____

_____

_____

Chair

University of California, San Diego

2019

DEDICATION

For KCL, my love.

EPIGRAPH

The irony of studying “discouragement” in graduate school has not escaped me.

TABLE OF CONTENTS

LIST OF FIGURES

ACKNOWLEDGEMENTS

I would like to acknowledge the members of Malinow lab for their support over the last 4 years. I would also like to acknowledge generous funding from the Kavli Foundation that partially supported my dissertation work.

Chapter 1, in full, is a reprint of the material as it appears in: Proulx CD*, Aronson SA*, Milivojevic D, Molina C, Loi A, Monk B, Shabel SJ, Malinow RM. (2017) A Neural pathway controlling motivation to exert effort. *Proceedings of the National Academy of Science. 115(22) 5792-5797.* The dissertation author was the co-primary investigator and co-author of this paper.

Chapter 2, in full, is in preparation for publication. Aronson, SR, Malinow, RM. "Individual Vesicular Events Activating GABA and AMPA Receptors onto Lateral Habenula Neurons." The dissertation author was the primary investigator and author of this publication.

VITA

2012 Bachelor of Arts, Oberlin College

2019 Doctor of Philosophy, University of California San Diego

PUBLICATIONS

Proulx CD*, Aronson SA*, Miliojevic D, Molina C, Loi A, Monk B, Shabel SJ, Malinow RM. (2018) A neural pathway controlling motivation to exert effort. *Proceedings of the National Academy of Science, 115(22),5792-5797*

ABSTRACT OF THE DISSERTATION

On the Lateral Habenula: Neurotransmitter Co-Release and a Neural Circuit Controlling Discouragement

by

Sage Ryan Aronson

Doctor of Philosophy in Neurosciences

University of California San Diego, 2019

Professor Roberto Malinow, Chair

Chapter 1: The neural mechanisms conferring reduced motivation, as observed in depressed individuals, is poorly understood. Here we examine in rodents if reduced motivation to exert effort is controlled by transmission from the lateral habenula (LHb, a nucleus overactive in depressed-like states) to the rostromedial tegmental nucleus (RMTg, a nucleus that inhibits dopaminergic neurons). In an aversive test wherein immobility indicates loss of effort, LHb→RMTg transmission increased during transitions into immobility; driving LHb→RMTg increased immobility; and inhibiting LHb→RMTg produced opposite effects. In an appetitive

test, driving LHb→RMTg reduced effort exerted to receive a reward, without affecting the reward's hedonic property. Notably, LHb→RMTg stimulation had an effect on only specific aspects of motor tasks and promoted avoidance, indicating that LHb→RMTg activity does not generally reduce movement but appears to carry a negative valence that reduce effort. These results indicate that LHb→RMTg activity controls the motivation to exert effort and may contribute to the reduced motivation in depression.

Chapter 2: Co-release of neurotransmitters has been detected in numerous brain regions under physiological and pathological conditions. However, if the opponent neurotransmitters γ-aminobutyric acid (GABA) and glutamate are normally released from single vesicles is not well established. A recent exhaustive study demonstrated that GABA and glutamate are released from individual presynaptic neurons originating at several nuclei targeting the lateral habenula (LHb). Their anatomical techniques indicated that GABA-containing and glutamate containing presynaptic vesicles are segregated. Here we use electrophysiology to characterize a different synaptic projection onto the lateral habenula, and find that the majority of individual quantal events contain a dual glutamate and GABA composition. The lateral habenula may therefore have multiple means to balance excitation and inhibition by co-released GABA and glutamate.

CHAPTER 1: A neural pathway controlling motivation to exert effort

Abstract

The neural mechanisms conferring reduced motivation, as observed in depressed individuals, is poorly understood. Here we examine in rodents if reduced motivation to exert effort is controlled by transmission from the lateral habenula (LHb, a nucleus overactive in depressed-like states) to the rostromedial tegmental nucleus (RMTg, a nucleus that inhibits dopaminergic neurons). In an aversive test wherein immobility indicates loss of effort, LHb→RMTg transmission increased during transitions into immobility; driving LHb→RMTg increased immobility; and inhibiting LHb→RMTg produced opposite effects. In an appetitive test, driving LHb→RMTg reduced effort exerted to receive a reward, without affecting the reward's hedonic property. Notably, LHb→RMTg stimulation had an effect on only specific aspects of motor tasks and promoted avoidance, indicating that LHb→RMTg activity does not generally reduce movement but appears to carry a negative valence that reduce effort. These results indicate that LHb→RMTg activity controls the motivation to exert effort and may contribute to the reduced motivation in depression.

Introduction

Depressive disorders cause significant morbidity and mortality in the human population (Ferrari et al., 2013). A number of potentially aberrant neural mechanisms have been characterized, which may reflect the multiplicity of depressive symptoms (Drevets et al., 2008; Airan et al., 2007; Berton and Nestler, 2006; Pittenger and Duman, 2007; Duman and Monteggia, 2006; Sahay and Hen, 2007; Parker et al., 2003; Mill and Petronis, 2007). While recent studies in humans (Morris et al., 1999; Sartorius et al., 2010; Ranft et al., 2009; Lawson et al., 2016; Carlson et al., 2013) and rodents (Amat et al., 2001; Yang et al., 2008; Caldecott-Hazard et al., 1988; Shumake and Gonzalez-Lima, 2003; Li et al., 2011; Shabel et al., 2014; Li

et al., 2013; Lecca et al., 2014; Lecca et al., 2016) suggest that excessive lateral habenula (LHb) activity may contribute to depression, the impact of LHb hyperactivity on an individual's level of motivation has not been examined.

Motivation can be defined as the propensity of an organism to exert effort to move towards a rewarding or away from an aversive stimulus (Salamone and Correa, 2012). The amount of effort an individual exerts to achieve a goal is believed to depend on a complex calculation of the cost required to perform a defined action and the perceived benefit gained from that action (Salamone and Correa, 2012). Maladaptive dysfunction in neural pathways encoding such information (e.g. if the cost of performing an action is overvalued or if the perceived benefit is undervalued) can lead to behavioral deficits such as the reduced motivation seen in depression (Treadway et al., 2012; Hollon et al., 2015). The specific neural pathways underlying such motivational deficits in depression are unknown.

The LHb, a predominantly glutamatergic nucleus, receives inputs from several limbic nuclei associated with motivational states (Kim and Lee, 2012; Stamatakis et al., 2016; Warden et al., 2012; Baker et al., 2016). It provides a major disynaptic inhibitory output, through the midbrain GABAergic rostromedial tegmental nucleus (RMTg), to monoaminergic centers (Barrot et al., 2012). In particular, the RMTg transmits reward-related signals from the LHb to dopamine neurons, which are suggested to play a central role in reinforcing or discouraging ongoing action (Barrot et al., 2012, Jhou et al., 2009). LHb→RMTg signals have been shown to promote active, passive and conditioned behavioral avoidance (Stamatakis et al., 2016). However, the relation between these signals and motivation have not been examined.

It is notable that monoaminergic output has been associated with increased motivated behavior and positive affective states (Hamid et al., 2015; Nestler and Carlezon, 2006). Increasing dopaminergic cell activity in the ventral tegmental area (VTA) increased motivated behavioral responses in a challenging task and their negative modulation decreased such responses (Tian et al., 2009). Additionally, negative modulation of the dopaminergic mesolimbic

system has revealed its crucial role in driving motivated behavioral responses. The impact of reduced mesolimbic system activity has been characterized as an inflation in the perceived cost of exerting effort leading to immobility (24). We thus reasoned that the LHb→RMTg pathway, by inhibiting monoaminergic centers, could control motivated behavior; in particular, we hypothesized that this pathway controls the motivation to exert effort.

Materials & Methods

Subjects

Male Sprague-Dawley rats, aged 6–8 weeks for virus injection and cannula placement and 10–12 weeks for behavioral and electrophysiological studies, were housed two per cage and kept on a 12/12 h light–dark cycle (lights on/off at 7:00/19:00). All procedures involving animals were approved by the Institutional Animal Care and Use Committees of the University of California, San Diego.

Virus preparation

The cDNA for the oChIEF variant of ChR2 was a gift from the lab of Dr. Roger Tsien. To make pAAV-hSyn-GFP, we PCR amplified eGFP from pEGFP-N1 vector and cloned it into pAAV-hSyn vector. pAAV-hSyn-eArch3.0-eYFP was kindly provided by Dr Karl Deisseroth (Stanford University). Recombinant AAVs were prepared as previously described (20). Viral titers were determined by real-time quantitative PCR methods and ranged from 1 x 10^{12} GC to 1 x 10^{13} GC.

Surgery

Rodents were anaesthetized with isoflurane for stereotaxic injection of AAVs into the lateral habenula (LHb) (AP: −3.4 mm; ML: +/-0.7 mm; DV: −4.85 to −5.0 mm). A total of 0.4–0.5 µl of virus was injected over an 8-10 min period. At the end of the injection, the pipet remained at the site for 5 min to allow for diffusion of the virus into the surrounding tissue. An optic fiber cannula was implanted just above the rostromedial tegmental nucleus (RMTg) (AP:

−7.0; ML: 1.6 mm; DV: −7.6 mm with an 8° angle) and secured to the skull with dental cement reinforced with surgical screws. For fiber photometry and optogenetic manipulations, rats were implanted with 400 μM and 200 μM diameter fibers, respectively. Rats were injected with 5 mg per kg carprofen (NSAID) after surgery.

Behavioral assays

Forced swim test (FST)

Rats were placed for 20 min in a cylinder of water (water temperature: 25–26 °C; cylinder: 30 cm in diameter and 40 cm high; water depth was set to prevent rats from touching the bottom with their hind limbs). Rat behavior during the FST was videotaped using a PC6EX3 infrared camera (SuperCircuits) at 3.74 frames/second. Mobility values were determined using Significant Motion Pixels (SMPs) analysis, an automated and unbiased methods to analyze animal motion (Kopec et al., 2007). Immobility in the FST, calculated from a 5 point smoothing of SMP data, correlated well with immobility estimated by a human observer (see Fig. 1.7). An immobility bout was defined as a period where values were < .8 SD of the mean lasting at least 2 seconds. In a few cases where an animal spent a significant fraction of time overall immobile, this threshold was adjusted to < .6 SD from the mean to better reflect the animal's behavior. Bouts were excluded if another identified bout fell within the baseline period or if the identified bout abutted the beginning or end of the trial. Movement data were cut into 10-second-long segments, with a 5 second baseline.

During the FST, rats were connected to an optic fiber patch cord. For photostimulation of oChIEF, we alternated 2 min periods without and with 25Hz optical stimulation (5ms optical pulse duration). The vast majority of LHb projection neurons target one midbrain aminergic nucleus (Bernard and Veh, 2012). Thus, stimulation experiments are not expected to affect LHb outputs other than to the RMTg. For experiments with eArch3.0-eYFP, constant green light was administered during photo-manipulation periods (2 min). While the use of eArch3.0 can increase spontaneous release, evoked release is reduced (Mahn et al., 2016). Our observation that the

opposite behavioral effects are seen in the experiments using eArch3.0, compared to use of oChIEF, suggests that evoked release is more important than spontaneous transmitter release in transmitting behaviorally relevant information at this synapse.

Open field

Rats were placed for 10 minutes in an arena (70 x 45 x 40 cm) and movement was videotaped from above using a PC6EX3 infrared camera (SuperCircuits) at 3.74 frames/second. Mobility was analyzed as described for the FST. Rats were connected to the laser and we alternated 2 min periods without and with 25Hz optical stimulation (5ms optical pulse duration). Periods with light stimulation were compared to the mean of flanking no-light periods to account for the general downward trend in mobility as a function of time.

Fiber Photometry (FP)

To record fluorescence signals from GCaMP6s, light from a 470 nm Light-Emitted Diode (LED) (Doric Lenses) was bandpass filtered (FB470-10, Thorlabs), collimated, reflected by a dichroic mirror (DMLP550R), and focused by a 20x objective (NA=0.4, Olympus, RMS20X). Excitation power was adjusted so as to get 35-50 µW of 470 nm light at the tip of the patch cord. Emitted GCaMP6s fluorescence was bandpass filtered (FF01-535/22-25, Semrock) and focused on the sensor of a CCD camera (Hamamatsu Orca). FP and movement data were aligned by simultaneously triggering the 470 nm LED and the start of the video capture. The end of the fiber was imaged at 27-42 hz (binned 8x). Mean value of a region of interest covering the cross-section of the fiber was calculated using ImageJ. These data were exported to MATLAB for further analysis. This experiment was replicated with two independent groups of rats. Data were pooled across experiments.

Correlation Analysis

FP data were corrected for heat-induced LED decay and photobleaching of GCaMP6s by fitting the data to a double-exponential decay curve. FP data were segmented about the onset of the previously determined bouts of immobility, binned so that the number of frames in a

FP segment equaled that of a movement segment, and the Pearson's correlation coefficient for each immobility bout was then calculated. For each rat, on average, we detected 42 +/- 8 immobility bouts. Data are presented as mean of the average R-score across rats.

Operant conditioning Training

Rats were trained and tested in a modular operant test chamber (Med Associates, St. Albans, VT). During the training and testing period, rats were kept on a restricted water schedule (2 h *ad libitum* daily). Rats were initially trained to associate a reward (20-30 µl of 10% sucrose) with a light above the dispenser receptacle before being trained to press a lever to obtain a reward (20-30 µl of 10% sucrose per lever press) in a fixed ratio (FR 1) schedule (one reward per lever press). Each FR1 session lasted 30 min and rats that successfully learned to press the lever to obtain rewards were selected for subsequent progressive ratio testing.

Progressive Ratio (PR) Lever Press

Rats were tested in a PR schedule as described elsewhere (Vollmayr et al., 2004). Briefly, sucrose rewards (20-30 µl of 7% sucrose) were earned with increasing number of lever presses. The final number of lever presses that produced a reward represented the breaking point value. All PR sessions were performed with rats connected to optic fiber cable; optical stimulation consisted of trains of 5 ms pulses delivered at 25Hz (1s on /1s off).

Sucrose preference test (SPT)

Rats were habituated to the two bottle (tap water or 1% sucrose) paradigm for 24 hours. During testing (30 min), water deprived (24 hours) rats were connected to an optic fiber cable. Testing alternated (daily) with or without optical stimulation trains (25Hz, 1s on/1s off). Consumption (water and sucrose solution) was calculated by weight. Total liquid consumed: amount of liquid per gram body weight; sucrose preference: sucrose solution consumed / total liquid consumed.

Real-Time Place Preference Test (RTPP)

RTPP was performed using previously described methods (Shabel et al., 2012). Preference scores were measured by taking time spent in context A minus time spent in context B divided by total time.

Rotarod

Rats were initially trained to remain on the rod (Ugo Basile Rota Rod) at low speed (5 rotations per minute, r.p.m.) for 5 min (day 1). Subsequently, rats connected to optic fiber cable alternated daily trials (without or with optical stimulation) on rotarod (20 r.p.m., day 1,2; 30 r.p.m., day 3,4). Optical stimulation was started 10 seconds before rats were placed on the rod. A minimum of a 30 min rest period was given between trials to minimize motor fatigue. day 4: alternating trials with rod speed ramped from 2-15 r.p.m in 20 sec and 2-30 r.p.m. in 30 sec. Test was stopped at 25 sec and 30 sec respectively if rats remained on the rod during and after the speed ramp.

In vivo recordings

Juxtacellular in vivo recordings were done as previously described (Nabavi et al., 2014). In brief, four weeks after injection of AAV-oChIEF-tdTomato into the LHb, rats were anesthetized and mounted on a custom made stereotaxic frame with an adjustable angle, to hold the head in a fixed position during the recording. The body temperature was regulated by a heating pad. Using aseptic surgical tools the skull was exposed and a hole (~3 mm) was made, centered at −7.0 mm AP and 2.6 mm ML. The recording electrode was a glass pipet (15–20 mΩ) filled with 0.5M NaCl. The recording electrode was connected to a Axopatch-1D amplifier. The signal was amplified (X1000), filtered (2K Hz) and digitized at 10 kHz using an Instrutech A/D interface. Data were acquired using custom software written in Igor Pro (Wavemetrics) and spikes were detected using a custom written MATLAB script. For optical stimulation, an optic fiber was glued to the glass pipet so that the tip of the fiber was 500 μm above the tip of the glass pipet to form an optrode. The optic fiber was connected to a 473 nm solid-state laser diode (Shanghai Laser & Optics Century Co.). The optrode was slowly lowered in at a 14° angle

following the start of stimulation. When spike activity was detected (DV: -7 to -7.8 from the top of the brain), photostimulation was evoked using 25Hz light pulses for 10 sec every 30 sec sweeps. All rats were perfused after the recordings and the position of the recording site verified.

Statistical Analyses

All statistical analyses were completed using MATLAB (Mathworks, 2016a) or GraphPad Prism 6 (GraphPad Software). Behavioral data were analyzed using two side paired or unpaired Student's t-test (indicated in text). For fiber photometry data, Pearson's correlations were performed using MATLAB.

Exclusion of animals or datapoints: Several rats were excluded post-hoc in the rare case that an optical fiber was misplaced or if expression of the construct of interest was off-target or low. Exclusion was done blind to both the animal's identification and the behavioral results. Fiber photometry recordings: During recordings of neural activity from axon terminals, while a rat is vigorously moving in the FST, a patch cord occasionally became loose from its connection with the rat. In such cases, portions of the recording sessions (or an entire recording session) were excluded. These determinations were made through a combined analysis of the motion-capture video and the fluorescence recordings.

Results

LHb→RMTg Activity Increases with Transitions to Immobility in the Forced Swim Test

To examine LHb→RMTg activity in a behaving animal, the LHb of rats was injected with an adeno-associated virus (AAV) genetically encoding the calcium indicator GCaMP6s (AAV-hSyn-GCaMP6s). An optical fiber was implanted over the RMTg to measure the activity of axon terminals from LHb→RMTg (Fig. 1A and Fig. 1.7; see Methods). Control rats received the same surgery, but were injected with an AAV encoding GFP (AAV-hSyn-GFP). Four weeks later, GCaMP6s expression was detected in cell bodies of the LHb and at the axon terminals of those

fibers in the RMTg (Fig. 1A). Changes in fluorescence, indicating changes in neural activity (Tian et al., 2009), were recorded with a custom-built fiber photometry system (see Methods, and (Kim et al., 2016). To assess motivation, rats were subjected to the forced swim test (FST (Porsolt et al., 1977)), an aversive inescapable environment in which a rat's effort is indicated by the persistence of its movement (Fig. 1B). Over the course of the test, the rat spends a larger fraction of time immobile. These periods of immobility can be used as a measure of reduced motivation in rodents (Warden et al., 2012; Tye et al., 2013; Rygula et al., 2005). The rats' behavior was captured using a digital camera and immobility bouts were determined using an unbiased MATLAB script that was validated against human scorers (Fig. 1.8; see Methods).

The onset of immobility bouts coincided with increased fluorescence signal (Fig. 1C and 1D), as indicated by a significant negative correlation between the rat's movement about the onset of an immobility bout and the neural activity of the LHb→RMTg (Fig. 1E, left; $R = -.27 \pm .01$; $p < 0.0001$ t-test; rat_n = 7; test_n = 12; bout_n = 298; see Methods and Supplemental Material). Such correlation was not observed in rats injected with AAV-GFP ($R = .05 \pm .02$; $p > .05$, t-test; rat_n = 2; test_n = 5; bout_n = 167). When the same analysis was made at periods of mobility (above threshold), no correlation was measured in rats expressing GCaMP6s (Fig. 1E, right; $R = .03 \pm .04$; $p > .05$ t-test; rat_n = 7; test_n = 12; bout_n = 424) or GFP ($R = -.02 \pm .06$; $p > .05$ t-test; rat_n = 2; test_n = 5; bout_n = 101). These findings support the view that increased neural activity in the LHb→RMTg correlates with reduced motivation to exert effort in an aversive context; furthermore, this correlation is not generally related to movement, as it occurs only during specific periods (i.e. at immobility threshold, when an animal would be expected to have low motivation).

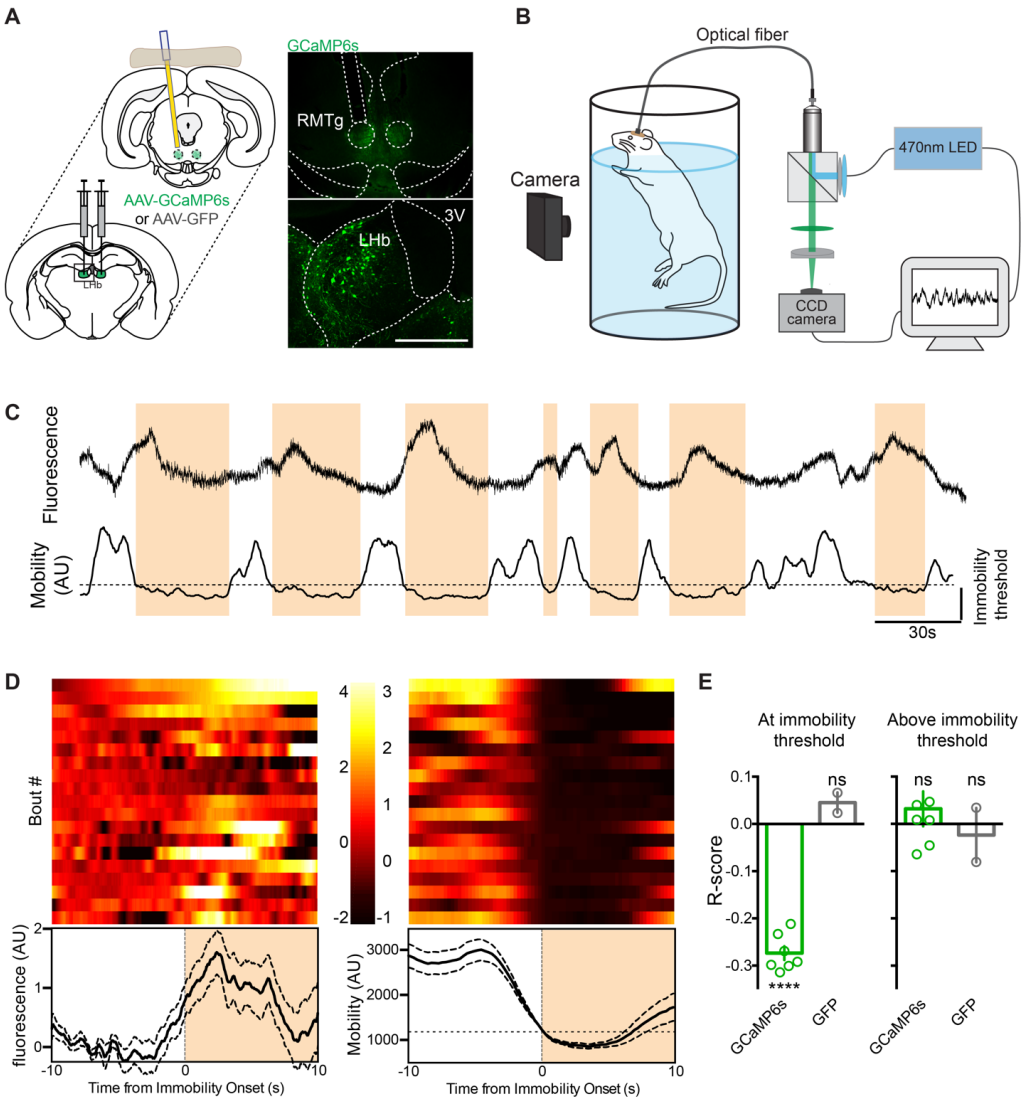

Figure 1.1. Activity of LHb→RMTg is coincident with immobility bouts in the FST.
a) AAV encoding GCaMP6s injected into LHb; 400um optical fiber implanted over the RMTg; diagram (left) and fluorescence images (right). Scale bar, 500 μM b) Diagram of recording setup. Video and CCD cameras captured rat mobility and changes in fluorescence in RMTg, respectively. c) Representative example of change in fluorescence (top) and mobility (bottom) during FST; immobility threshold indicated. Scale bar, Y-axis: top and bottom, AU. d) Representative examples (top) and mean ± SEM (bottom) of change in fluorescence (left) and mobility (right), aligned to onset of immobility bout. e) Graph of correlation (Pearson's) between fluorescence and mobility for rats (individual, circles; mean, bar) expressing indicated constructs, aligned about onset of immobility bouts (left) or during periods of mobility (right). For all figures: * p< .05, ** p< 01, *** p< .001, **** p< .0001; ns, not significant; paired Student's t-test, unless otherwise indicated.

Driving LHb→RMTg Increases Immobility in the Forced Swim Test

To test the hypothesis that the activity of the LHb→RMTg is sufficient to reduce the motivation to exert effort, the LHb was injected with an AAV encoding a light-dependent excitatory opsin oChIEF (Lin et al., 2009) fused to the red fluorescent protein tdTomato (AAV-hSyn-oChIEF-tdTomato) or a control fluorophore (AAV-hSyn-tdTomato), and an optical fiber was implanted over the RMTg (Fig. 1.2A and Fig.S3). Single-unit recordings in anesthetized rats confirmed that brief 5 ms pulses of blue light (~15 mW at optical fiber tip) delivered at 25 Hz was sufficient to drive postsynaptic activity in RMTg neurons (Fig. 1.10).

Rats were subjected to 20 minute FST sessions as used in fiber photometry recordings with each session consisting of alternating 2 minute epochs with and without unilateral 25 Hz optical stimulation (Fig. 1.2B). Stimulation of the LHb→RMTg was sufficient to decrease a rat's mobility during 2 minute epochs, as compared to the average mobility in the preceding and proceeding non-stimulation epochs (Fig. 1.2C; 3300 ± 100 smp [significant motion pixels (43)], no-light vs 2700 ± 100 smp, light; $p < .001$). There was no significant effect of stimulation on rats' average mobility above the immobility threshold, suggesting that stimulation did not affect a rat's ability to move nor the vigor of movement when the rat was not immobile (Fig. 1.2D; 3500 ± 100 smp, no-light vs 3400 ± 100 smp, light; $p > .05$). Rather, the overall effect of stimulation on mobility was mostly due to an increase in the fraction of time a rat spent below the mobility threshold (Fig. 1.2E; .15 ± .01, no-light vs .32 ± .02, light; $p < .001$). We observed that these immobility events occurred more often (18 ± 3 events, no-light vs 33 ± 1 events, light; $p<0.001$) and were longer in duration (3.7 ± 0.6 sec, no-light vs 5.6 ± 0.3 sec, light; $p<0.05$) during activation of the LHb→RMTg. Stimulation had no significant effect on the mobility of control rats expressing tdTomato (Fig. 1.2C-E; Mobility, 3300 ± 70 smp, no-light vs 3300 ± 80 smp, light; $p > .05$; Mobility above threshold, 3620 ± 60 smp, no-light vs 3620 ± 80 smp, light; $p > .05$; Fraction immobility, .19 ± .01, no-light vs .17 ± .02, light; $p > .05$), with no change in the number (30 ± 4

events, no-light vs 26 ± 3 events, light; $p>0.05$) or the duration (3.4 ± 0.3 sec, no-light vs 6.9 ± 2.8 sec, light; $p>0.05$) of immobility events. These results support the view that stimulation of the LHb→RMTg neural pathway is sufficient to reduce motivation to exert effort in an aversive context.

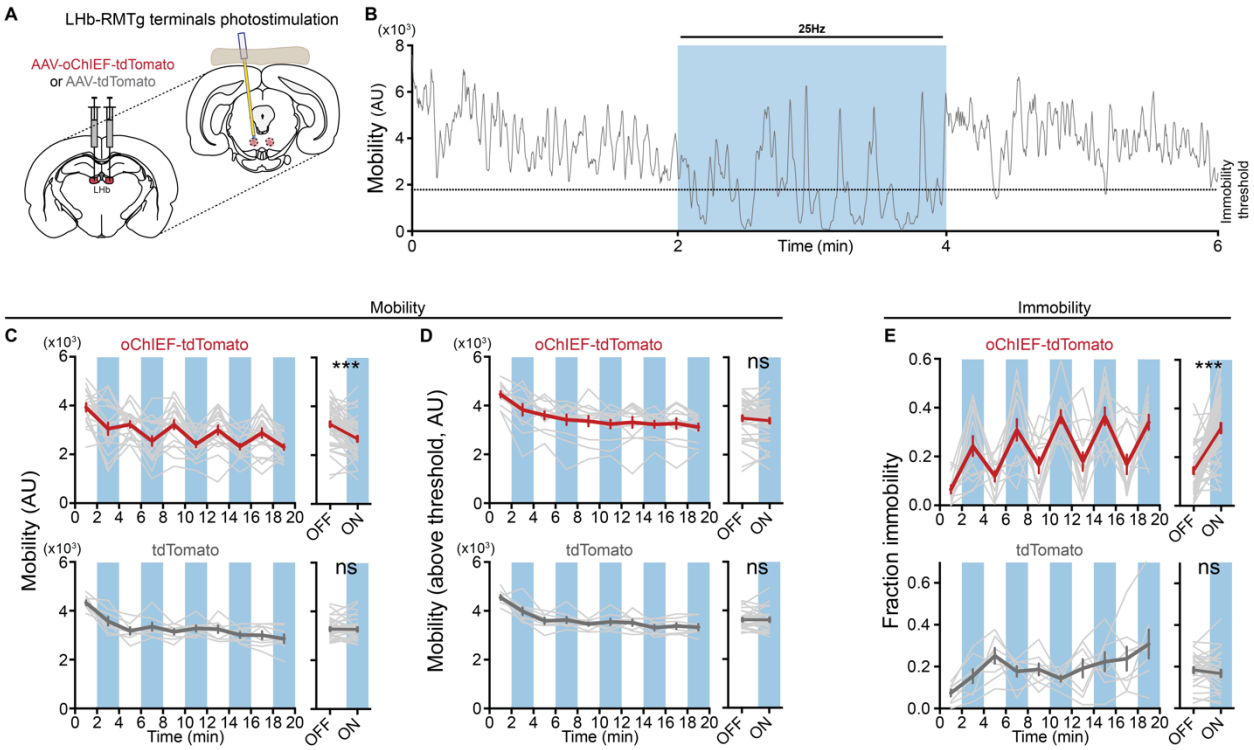

Figure 1.2. Stimulation of LHb→RMTg increases immobility in FST.
a) AAV encoding the light-sensitive cation channel oChIEF-tdTomato (n=13) (or tdTomato alone, n=7) injected into the LHb; 200um optical fiber implanted over RMTg. b) Representative example of change in mobility during light delivery (blue). c-e) Top: c, left, plot of mean mobility (gray, individual rats; red, mean ± SEM) during periods of light (blue) or no light (white). Right, mean (± SEM) for indicated periods. d) Same as c for mobility values above immobility threshold. e) Same as c for time spent immobile. Bottom c-e, same as above for rats expressing tdTomato.

Inhibiting LHb→RMTg Reduces Immobility in the Forced Swim Test

To test the hypothesis that activity in the LHb→RMTg is necessary to drive immobility in the same aversive swim test, rats were injected in the LHb with an AAV encoding the light-dependent proton pump eArch3.0 fused to a yellow fluorescent protein (AAV-hSyn-eArch3.0-eYFP) or with GFP (AAV-EF1✔-GFP) as control. 200 μm optical fibers were implanted over the RMTg (Fig. 1.3A and Fig. 1.11). As above, rats were examined during a 20 minute swim session with alternating 2 minute epochs of no-light and constant green light. When light was applied, a rat's mobility in an epoch with light was significantly higher than the average mobility of the flanking epochs without light (Fig. 1.3B-C; 3620 ± 90 smp, no-light vs 3770 ± 90 smp, light; $p < .05$). Furthermore, light delivery decreased the fraction of time the rat spent immobile (Fig. 1.3E; .25 ± .02, no-light vs .17 ± .02, light; $p < .01$). We observed that these immobility events occurred less often (33 ± 1 events, no-light vs 22 ± 2 events, light; $p<0.05$) and were shorter in duration (4.7 ± 0.2 sec, no-light vs 3.8 ± 0.1 sec, light; $p<0.05$) when light was delivered to the RMTg. No significant change was observed in rats expressing GFP (Fig. 1.3C-E; Mobility, 3360 ± 90 smp, no-light vs 3400 ± 100 smp, light; $p > .05$; Mobility above threshold, 3710 ± 80 smp, no-light vs 3700 ± 100 smp, light; $p > .05$; Fraction immobility, .21 ± .02, no-light vs .20 ± .01, light; $p > .05$) with no change in the number of events (33 ± 2 events, no-light vs 31 ± 4 events, light; $p>0.05$) nor their duration (3.8 ± 0.3 sec, no-light vs 3.4 ± 0.2 sec, light; $p>0.05$).

These results are opposite compared to those observed with blue light activation of oChIEF, supporting the views that green light delivery to eArch3.0-expressing terminals inhibits their activity (Mattis et al., 2012; Vento et al., 2017) and that LHb→RMTg activity is necessary to produce the normal level of immobility in the aversive context of the FST.

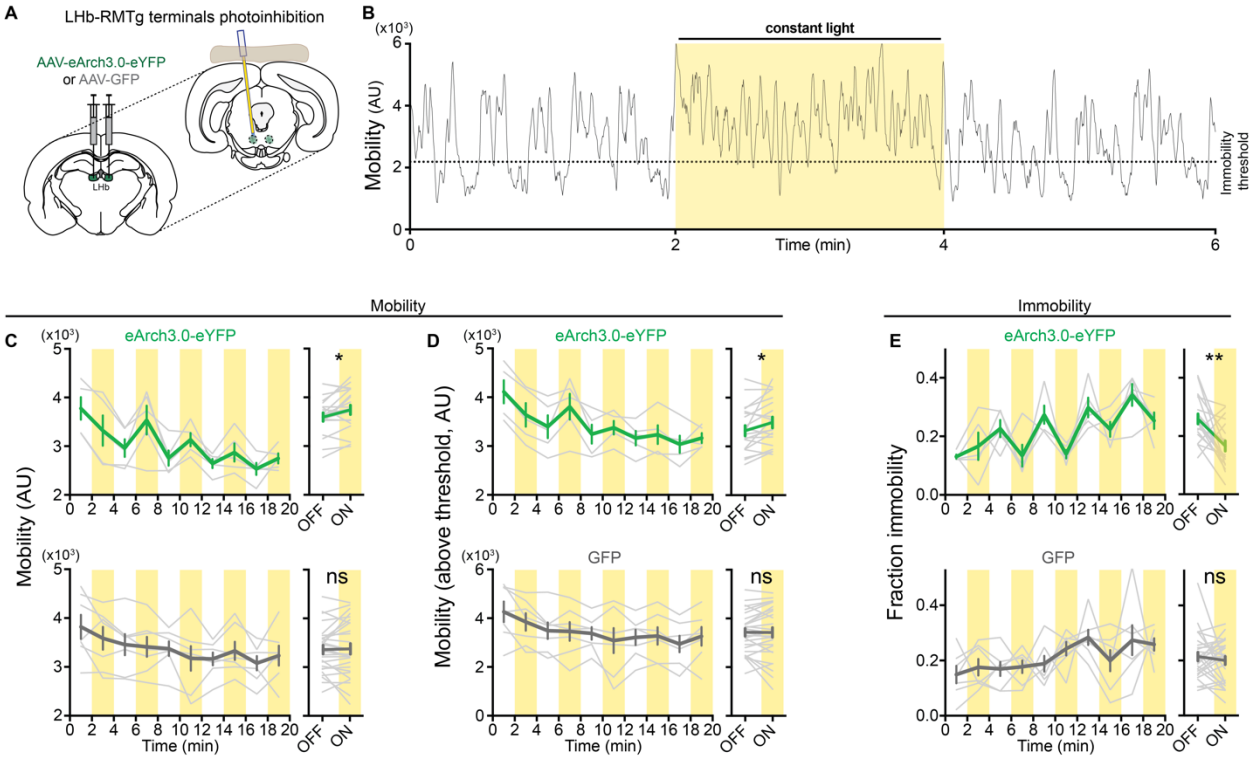

Figure 1.3. Reducing LHb→RMTg activity decreases immobility in FST
a) AAV encoding the hyperpolarizing proton pump eArch3.0 (n=5) or GFP (n=7) injected into the LHb; 200um optical fiber implanted over the LHb. b) Representative example of change in mobility during light delivery (yellow). Top: c, left, plot of mean mobility (gray, individual rats; green, mean ± SEM) during periods of light (yellow) or no light (white). Right, mean (± SEM) for indicated periods. d) Same as c for mobility values above immobility threshold. e) Same as c for time spent immobile. Bottom c-e, same as above for rats expressing GFP.

Activating LHb→RMTg Reduces Effort Exerted to Gain Rewards in an Appetitive Task

To examine if increased activity at the LHb→RMTg was sufficient to decrease motivation in an appetitive context, rats were tested in a progressive ratio (PR) operant task, a common behavioral test to evaluate motivation in rodents (Aberman et al., 1988). In this test, increasing work (more lever presses) is required to receive a reward as trials proceed. The maximal work a rat exerts to receive a reward, the breaking point (BP), is used as a measure of its motivation (Fig. 1.4A).

We trained rats injected with AAV-hSyn-oChIEF-tdTomato in the LHb to press a lever to obtain a sucrose reward. After training, we tested rats with a PR schedule of reinforcement (see Methods). In alternating sessions (one session per day), rats were or were not exposed to blue light through an optical fiber (trains of 25 Hz for one second every two seconds) during the entire session. With stimulation, rats' BPs were significantly reduced by more than 40% compared to non-stimulation sessions (Fig. 1.3Bi; BP no-light 35 ± 4, BP light 21 ± 3; $p < 0.001$). This indicates that driving LHb→RMTg activity is sufficient to reduce the work performed by a rat to receive a reward. LHb→RMTg stimulation significantly increased the time between receiving a reward and the subsequent lever press (Fig. 1.4Bii; 36 ± 5 sec, no-light vs 67 ± 12 sec, light; $p<0.05$). Interestingly, the time between lever presses was unaffected (Fig. 1.4Biii; 0.85 ± 0.04 sec, no-light vs 0.88 ± 0.05 sec, light; $p>0.05$), suggesting that once a threshold motivation to work was achieved, the vigor of a rat's performance was not modified. Notably, stimulation did not affect a rat's preference for sucrose over water (sucrose preference test ; SPT) indicating that the hedonic value of the reward was unaffected by stimulation (Fig. 1.4C; 84 ± 4 %, no-light vs 73 ± 6, light; $p > 0.05$). Additionally, LHb→RMTg activation did not reduce thirst as revealed by the total liquid consumed (Fig. 1.4C; .037 ± .002, no-light vs .032 ± .003; $p > 0.05$). These results indicate that the motivation to exert effort to receive a reward, rather than the value of the reward or the ability to perform the task, is affected by LHb→RMTg activation.

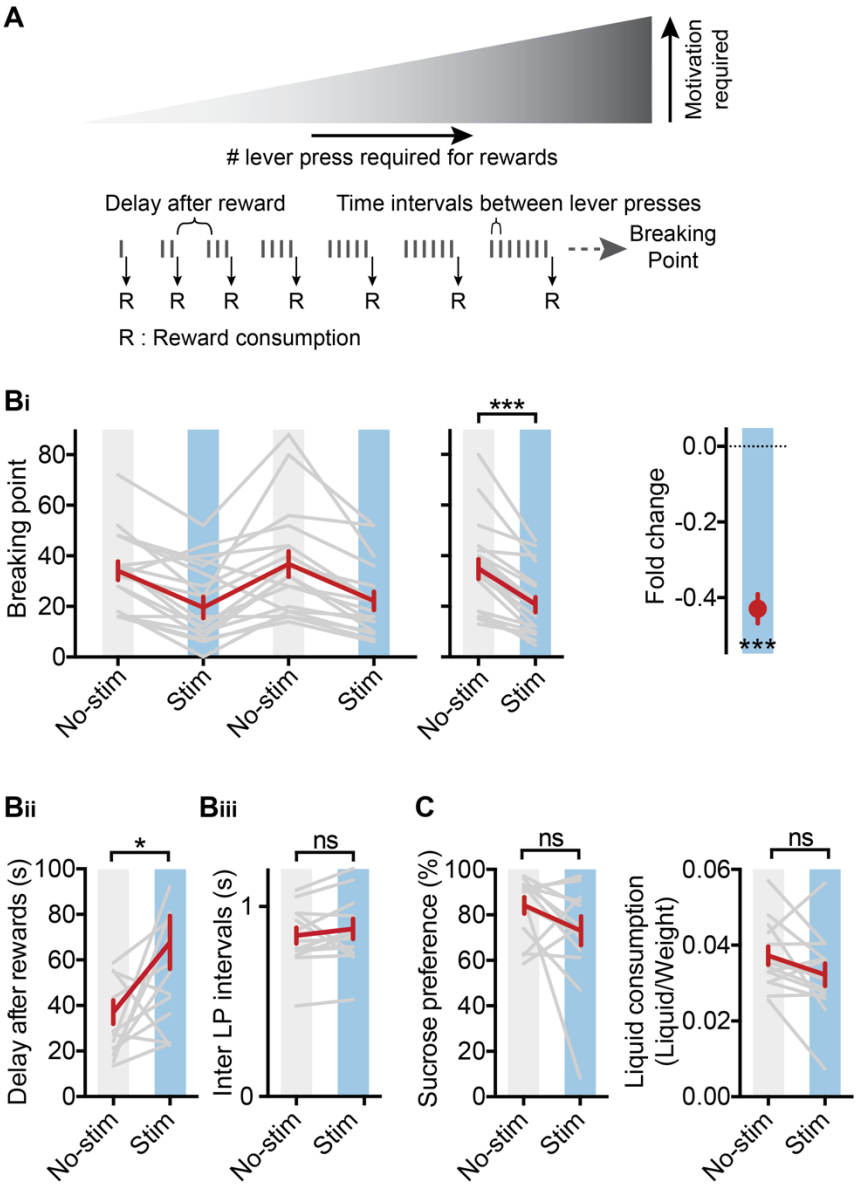

Figure 1.4. Stimulation of LHb→RMTg reduces motivation to receive reward but not reward value. a) Diagram of progressive-ratio reinforcement schedule; see methods. b) plots of i, breaking point, ii, delay after rewards and iii, interval between lever presses for mean of daily trials (i, left) or indicated conditions (i, middle; ii, iii) or fold change by stimulation (i, right); gray, individual rats; red, mean ± SEM. c) plots of sucrose preference (left) and total liquid consumed (right) for indicated conditions during sucrose preference test, see methods. Same rats as used in Fig. 1.2.

Activating LHb→RMTg during an open field test

We next tested animals in the open field (OF) test (Tye et al., 2013), normally use to determine if a manipulation has non-specific effects on movement. Rats expressing oChIEF-tdTomato or the control fluorophore tdTomato were placed in an open field and movement were monitored during a 10 min period during in which alternating 2 minute epochs with and without unilateral 25 Hz optical stimulation were delivered (Fig. 1.5). When light was applied, a rat's mobility in an epoch with light was significantly lower than that of the flanking epochs without light (Fig. 1.5). Both low and high levels of movement were affected by light (Fig. 1.5A-C; Mobility, 940 ± 40 smp, no-light vs 490 ± 60 smp, light; $p < .001$; Mobility above threshold, 1240 ± 40 smp, no-light vs 760 ± 70 smp, light; $p < .001$; Fraction immobility, .28 ± .03, no-light vs .46 ± .04, light; $p < .001$). Stimulation had no significant effect on the mobility of control rats expressing tdTomato (Fig. 1.5A-C; Mobility, 660 ± 70 smp, no-light vs 750 ± 80 smp, light; $p > .05$; Mobility above threshold, 1000 ± 80 smp, no-light vs 1000 ± 100 smp, light; $p > .05$; Fraction immobility, .40 ± .03, no-light vs .26 ± .03, light; $p > .05$).

While the OF test has been used to measure basic motor function, this test is also a measure of a rat's motivation to explore an environment (Archer et al., 1973; Roth and Katz, 1979). Since there was no effect of LHb→RMTg stimulation on supra-threshold mobility in the FST nor on the inter-lever-press interval in the PR test, the more parsimonious interpretation would be that the effect of such stimulation on the OF test is due to reduced motivation to explore and not an effect on general motor function.

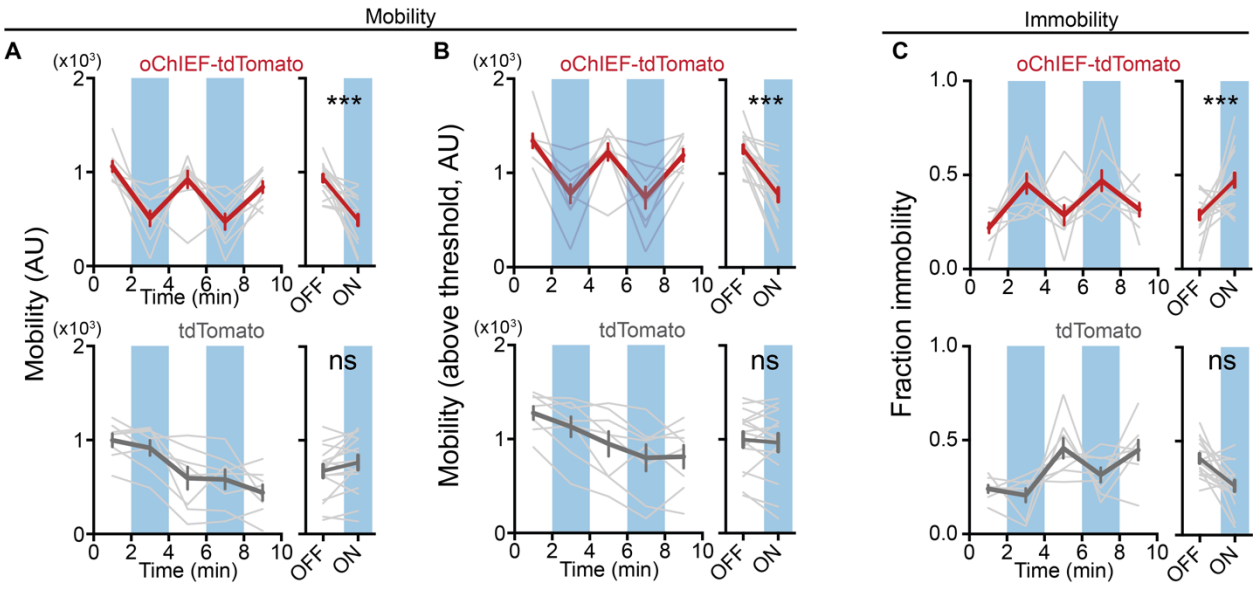

Figure 1.5. Stimulation of LHb→RMTg increases immobility in the open field.
a-c) Top: a, left, plot of mean mobility for rats expressing oChIEF (gray, individual rats; red, mean ± SEM) during periods of light (blue) or no light (white). Right, mean (± SEM) for indicated periods. b) Same as a for mobility values above immobility threshold. c) Same as a for time spent immobile. Bottom a-c, same as above for rats expressing tdTomato. Same rats as used in Fig. 1.2 and 4.

Activating LHb→RMTg has No Effect on Motor Coordination and is Aversive

As a further test to distinguish between an effect of LHb→RMTg activity on the motivation to move rather than an effect on general motor function, rats injected with AAV-oChIEF-tdTomato, which had already been tested on the FST (see Fig. 1.2), were tested on the rotarod, a task requiring quick and coordinated movements. After an initial training period, rats' latencies to fall were measured under a number of conditions (slow or fast constant speed, slow or fast ramping speed) (Fig. 1.6A). Under no condition did LHb→RMTg stimulation have a significant effect on rats' latencies to fall (Fig. 1.6B; 20 rpm, 177 ± 21 sec, no-light vs 153 ± 23 sec, light; $p > .05$; 30 rpm, 59 ± 18 sec, no-light vs 53 ± 22 sec, light; $p > .05$; ramp 2-15 rpm, 18 ± 1.2 sec, no-light vs 17 ± 1.3 sec, light; $p > .05$; ramp 2-30 rpm, 26 ± 1.7 sec, no-light vs 26 ± 1.9 sec, light; $p > .05$). Notably, these animals had shown specific deficits in the FST. This indicates that LHb→RMTg stimulation does not have a generalized effect on motor activity, but rather only under specific conditions.

Finally, we asked whether stimulation of the LHb→RMTg was aversive, as would be expected for the experience of reduced motivational states (Bromberg-Martin et al., 2010). In this test (the real-time place preference task), rats are placed in a box with two compartments. After an initial habituation period, rats received optical stimulation (25 Hz) only when they were present in one compartment. Rats expressing oChIEF actively avoided the compartment paired with stimulation. Stimulation had no significant effect on control rats expressing tdTomato. These results are suggesting that overactivity of the LHb→RMTg is aversive (Fig. 1.5C) (Stamatakis and Stuber, 2012).

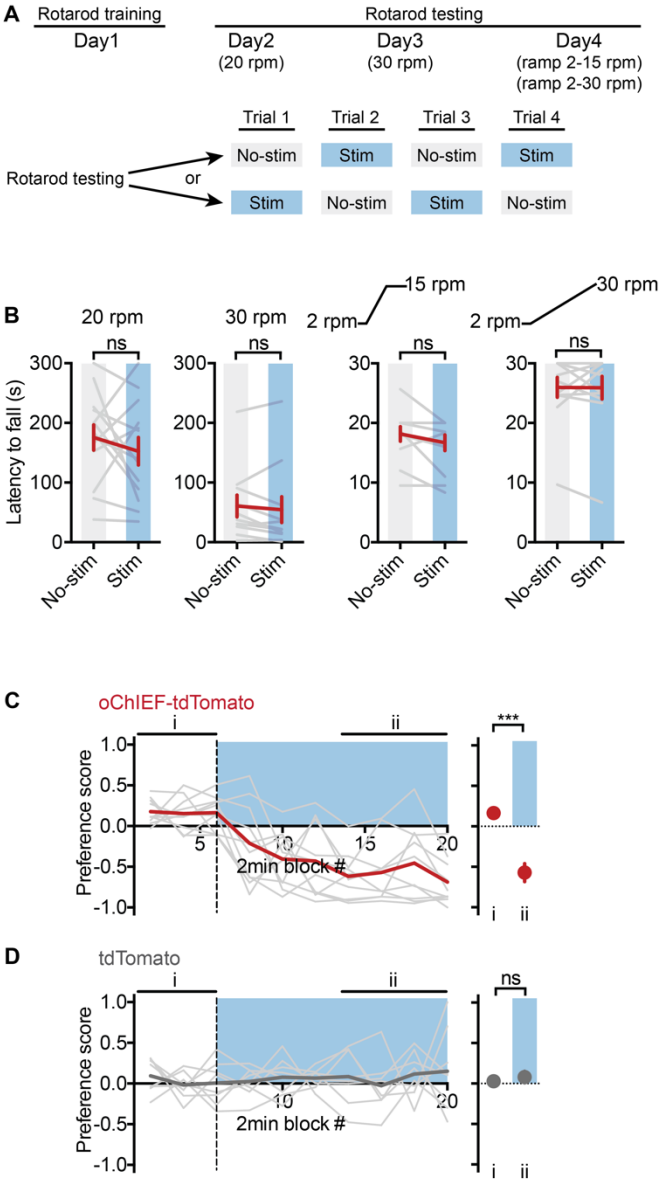

Figure 1.6. Stimulation of the LHb→RMTg had no effect on motor coordination and is aversive a) Diagram of rotarod test (see methods) schedule. b) plot of latency to fall for indicated conditions. c,d) Real-time place preference test. Left, plots of preference score (gray, individual rats; red, mean) for indicated conditions. Right, mean for values during indicated periods (i, ii); blue, period of light stimulation while rat in unpaired (above x-axis) or paired (below x-axis) side of box. Same rats as used in Figures 2 and 4.

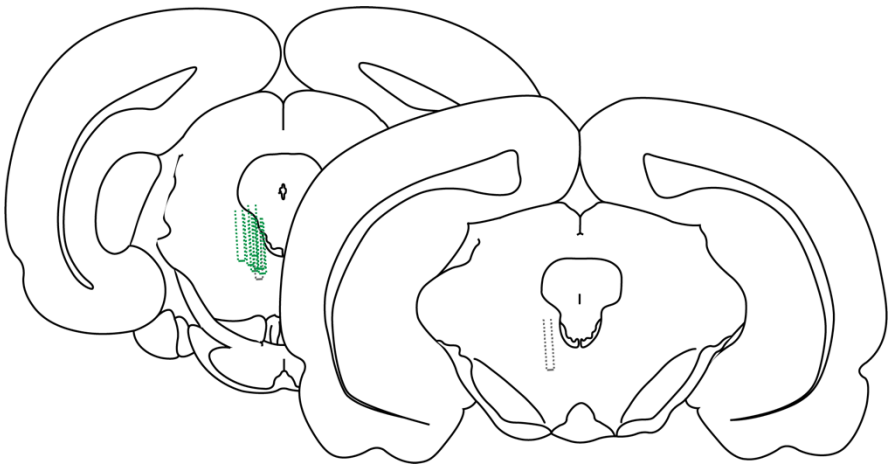

Figure 1.7. Location of optical fibers placement in the RMTg of rats injected with AAV-hSyn-GCaMP6s (depicted in green) or AAV-hSyn-eGFP (depicted in grey).

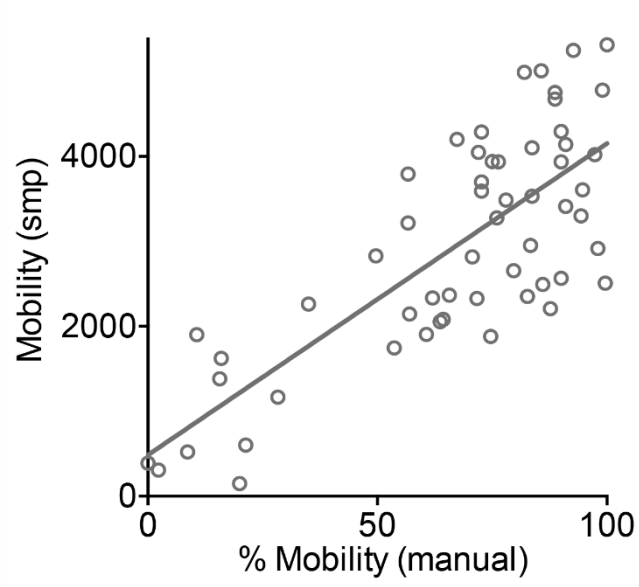

Figure 1.8. SMPs is an accurate predictor of mobility in the FST
Plot of SMPs vs mobility determined by a human observer. Each open circle is a different rat tested in the FST. $R = 0.77$, $p < 0.0001$

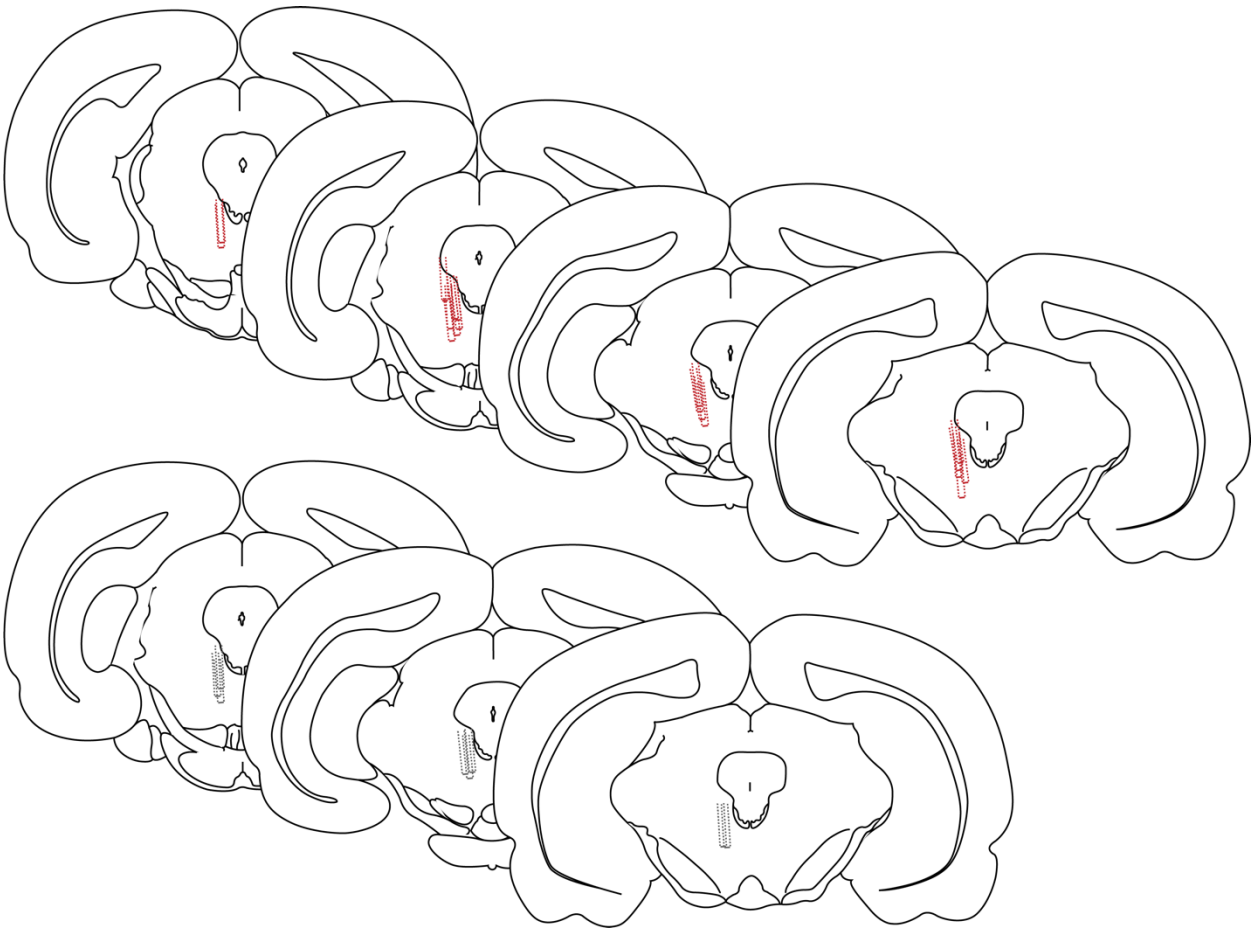

Figure 1.9. Location of optical fibers placement in the RMTg of rats injected with AAV-hSyn-oChIEF-tdTomato (depicted in red) and AAV-hSyn-tdTomato (depicted in grey).

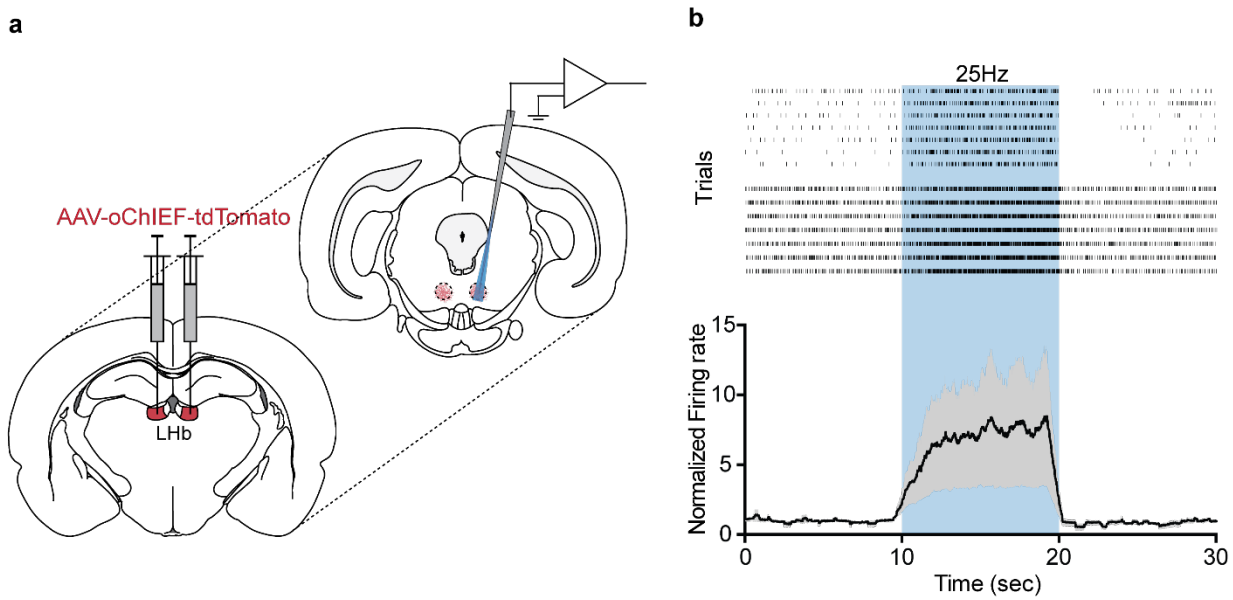

Figure 1.10. Optogenetic stimulation of the LHb-RMTg pathway increases firing of RMTg neurons

a) Diagram of AAV encoding the light-sensitive cation channel oChIEF-tdTomato injected into the LHb; juxtacellular recordings of RMTg neurons. b) Top, rasterplots of juxtacellular recordings of single RMTg neurons (top, two examples) in anesthetized rats. Lower, plot of average normalized firing (mean, line; SEM, gray shade; n=6). Fold increase in firing during stimulation of LHb terminals, 8.5 ± 3.5, $p<0.05$, paired Student's t-test.

Figure 1.11. Location of optical fibers placement in the RMTg of rats injected with AAV-hSyn-eArch3.0-eYFP (depicted in yellow) and AAV-hSyn-eGFP (depicted in grey).

Discussion

Major depression is a leading cause of disability worldwide (Ferrari et al., 2013). It encompasses a heterogeneous set of disorders with distinct features (e.g. depressed mood, anhedonia, altered weight and/or sleep, fatigue, guilt, etc.). Abnormalities in several brain regions, such as the ventral tegmental area, the nucleus accumbens, and, more recently, the LHb, have been linked to depression (Drevets et al., 2008; Airan et al., 2007; Berton and Nestler, 2006, Proulx et al., 2014).

A deficit in motivation is a central symptom of depression as well as other psychiatric disorders (Treadway and Zald, 2011; Salamone et al., 2014). This deficit could be the result of inflating the perceived cost of the effort required to achieve a goal or undervaluing the potential benefit of achieving a reward (Salamone and Correa, 2012; Treadway et al., 2012, Hollon et al., 2015). In either case, a deficit in motivation suggests an abnormality in the functional link between brain regions encoding reward-related events and those controlling motivated behavior. Anatomically, the LHb is well suited to fill this role as it receives afferents from brain nuclei signaling reward-related events and provides negative signals to aminergic centers known to control motivated behaviors (Stamatakis et al., 2016; Warden et al., 2012; Baker et al., 2016, Kim and Lee, 2012). Because the RMTg is an important output target of the LHb that inhibits dopaminergic centers, we tested whether the projection from the LHb to the RMTg can control motivated behavior.

In an initial set of experiments, we examined if the motivation to exert effort in an aversive environment is controlled by the LHb→RMTg. We find that this pathway displays increased activity coinciding with the animal's entry into states of immobility in the FST - states that are classically described as 'behavioral despair' and are a measure of reduced motivation in an aversive and energetically demanding environment (Warden et al., 2012; Tye et al., 2013; Rugula et al., 2005). Notably, activity in this pathway did not correlate during periods of mobility, suggesting that this pathway doesn't simply control movement. Driving or inhibiting this

pathway increases or decreases, respectively, a rat's mobility, specifically by changing the frequency and duration of inactive states with no effect on its ability to move vigorously. Combined, these data establish a causal relationship between activity of the LHb→RMTg pathway and immobility, supporting the view that this pathway controls the motivation to sustain effort in an aversive context. Interestingly, stimulation of medial prefrontal cortex (mPFC) axons terminating in the LHb also reduced mobility in the FST (Warden et al., 2012). Our results suggest that mPFC→LHb inputs may target LHb neurons that project to the RMTg.

We also tested if the motivation to exert effort in a rewarding environment is controlled by the LHb→RMTg. Given the complexity of the brain circuitry known to encode reward and aversion, where specific circuit components have been identified for each (Hu, 2016), the motivation to exert effort in these different contexts could be mediated by separate or overlapping mechanisms. Here we show that activation of the LHb→RMTg pathway reduced the motivation to work for a reward in an appetitive operant task suggesting at least some overlapping neural pathways controlling motivation in both aversive and appetitive contexts.

The effects observed in our behavioral tasks measuring the impact of LHb→RMTg stimulation on motivation are unlikely to be caused by a general reduction in mobility, as suggested by its effect in the OF test. This conclusion is supported by several observations: LHb→RMTg stimulation 1) produced no change in mobility above the immobility threshold in the FST; 2) did not affect the inter-lever press interval in the PR task; 3) did not affect the total liquid consumed in the SPT; 4) had no effect during the rotarod test; and 5) drove, rather than inhibited, movement in the real-time place preference test. Furthermore, LHb→RMTg activity correlated with transitions into immobility, but not generally with movement. Taken together, these data support the view that increasing LHb→RMTg activity does not have a general effect on motor behavior, but rather controls motivation to exert effort. We propose that the effects seen in the OF test may be due to the nature of the test. Unlike the other test, which showed no effects (rotarod) or effects only on specific aspects (FST, PR), the OF test requires little

motivation and provides little rewards. Under these conditions, reduced motivation may have greater impact.

Our results are consistent with pharmacological and dopamine depletion manipulations, which have been shown to reduce the amount of effort made in challenging or energetically demanding conditions, and to decrease spontaneous (non-goal oriented) locomotor function (e.g. open field); while leaving intact some motor behaviors (Salamone and Correa, 2012; Treadway et al., 2012; Baldo et al., 2002). Other studies examining inputs to, or outputs from, the LHb, are also consistent with LHb→RMTg activity reducing motivation (Kim and Lee, 2012; Stamatakis et al., 2016; Warden et al., 2012; Baker et al., 2016). Our results suggest that this pathway provides important negative modulation of dopamine neurons to gate effort exerted in challenging conditions.

In summary, our data indicate that activity of neurons that project from the LHb to the RMTg control the motivation to perform behaviors requiring effort, irrespective of whether those behaviors are directed toward escaping an aversive condition or toward acquiring a reward. Aberrant over-activity of this pathway, previously examined in other contexts (Stamatakis and Stuber, 2012; Knowland et al., 2017), may be responsible for some of the motivational deficits seen in depression.

Chapter 1, in full, is a reprint of the material as it appears in: Proulx CD*, Aronson SA*, Milivojevic D, Molina C, Loi A, Monk B, Shabel SJ, Malinow RM. (2017) A Neural pathway controlling motivation to exert effort. *Proceedings of the National Academy of Science. 115(22) 5792-5797.* The dissertation author was the co-primary investigator and co-author of this paper.

References

Aberman JE, Ward SJ, Salamone JD (1998) Effects of Dopamine Antagonists and Accumbens Dopamine Depletions on Time- Constrained Progressive-Ratio Performance. *psychology biochemistry and behavior* 61(4):341–348.

Airan RD, Meltzer LA, Roy M, Gong Y, Chen H, Deisseroth K. High-speed imaging reveals neurophysiological links to behavior in an animal model of depression.Science. 2007 Aug 10;317(5839):819-23. Epub 2007 Jul 5.

Amat J, Sparks PD, Matus-Amat P, Griggs J, Watkins LR, Maier SF. The role of the habenular complex in the elevation of dorsal raphe nucleus serotonin and thechanges in the behavioral responses produced by uncontrollable stress. Brain Res.2001 Oct 26;917(1):118-26.

Archer J (1973) Tests for emotionality in rats and mice: A review. *Animal Behaviour* 21:205–235.

Baker PM, Jhou T, Li B, Matsumoto M, Mizumori SJ, Stephenson-Jones M, Vicentic A. The Lateral Habenula Circuitry: Reward Processing and Cognitive Control. J. Neurosci. 2016 Nov 9;36(45):11482-11488. Review.

Baldo BA, Sadeghian K, Basso AM (2002) Effects of selective dopamine D1 or D2 receptor blockade within nucleus accumbens subregions on ingestive behavior and associated motor activity. *Behavioural Brain Research*:165–177.

Barrot M, Sesack SR, Georges F, Pistis M, Hong S, Jhou TC. Braking dopamine systems: a new GABA master structure for mesolimbic and nigrostriatal functions. J Neurosci. 2012 Oct 10;32(41):14094-101. doi: 10.1523/JNEUROSCI.3370-12.2012. Review.

Bernard R, Veh RW (2012) Individual neurons in the rat lateral habenular complex project mostly to the dopaminergic ventral tegmental area or to the serotonergic raphe nuclei. *J Comp Neurol* 520(11):2545–2558.

Berton O, Nestler EJ (2006) New approaches to antidepressant drug discovery: beyond monoamines. *Nat Rev Neurosci* 7(2):137–151.

Bromberg-Martin ES, Matsumoto M, Hikosaka O (2010) Dopamine in Motivational Control: Rewarding, Aversive, and Alerting. *Neuron* 68(5):815–834.

Caldecott-Hazard S, Mazziotta J, Phelps M (1988) Cerebral correlates of depressed behavior in rats, visualized using 14C-2-deoxyglucose autoradiography. *J Neurosci* 8(6):1951–1961.

Carlson PJ, Diazgranados N, Nugent AC, Ibrahim L, Luckenbaugh DA, Brutsche N,

Herscovitch P, Manji HK, Zarate CA Jr, Drevets WC. Neural correlates of rapid antidepressant response to ketamine in treatment-resistant unipolar depression: a preliminary positron emission tomography study. Biol Psychiatry. 2013 Jun 15;73(12):1213-21. doi: 10.1016/j.biopsych.2013.02.008. Epub 2013 Mar 27.

Drevets WC, Price JL, Furey ML (2008) Brain structural and functional abnormalities in mood disorders: implications for neurocircuitry models of depression. *Brain Struct Funct* 213(1-2):93–118.

Duman RS, Monteggia LM (2006) A Neurotrophic Model for Stress-Related Mood Disorders. *Biol Psychiatry* 59(12):1116–1127.

Ferrari AJ, Charlson FJ, Norman RE, Patten SB, Freedman G, Murray CJ, Vos T, Whiteford HA. Burden of depressive disorders by country, sex, age, and year: findings from the global burden of disease study 2010. PLoS Med. 2013bNov;10(11):e1001547. doi: 10.1371/journal.pmed.1001547. Epub 2013 Nov 5.

Hamid AA, Pettibone JR, Mabrouk OS, Hetrick VL, Schmidt R, Vander Weele CM, Kennedy RT, Aragona BJ, Berke JD. Mesolimbic dopamine signals the value of work. Nat Neurosci. 2016 Jan;19(1):117-26. doi: 10.1038/nn.4173. Epub 2015 Nov 23.

Hollon NG, Burgeno LM, Phillips PEM (2015) Stress effects on the neural substrates of motivated behavior. *Nat Neurosci* 18(10):1405–1412.

Hong S, Jhou TC, Smith M, Saleem KS, Hikosaka O (2011) Negative reward signals from the lateral habenula to dopamine neurons are mediated by rostromedial tegmental nucleus in primates. *J Neurosci* 31(32):11457–11471.

Hu H (2016) Reward and Aversion. *Annu Rev Neurosci* 39(1):297–324.

Jhou TC, Fields HL, Baxter MG, Saper CB, Holland PC (2009) The Rostromedial Tegmental Nucleus (RMTg), a GABAergic Afferent to Midbrain Dopamine Neurons, Encodes Aversive Stimuli and Inhibits Motor Responses. *Neuron* 61(5):786–800.

Kim CK, Yang SJ, Pichamoorthy N, Young NP, Kauvar I, Jennings JH, Lerner TN, Berndt A, Lee SY, Ramakrishnan C, Davidson TJ, Inoue M, Bito H, Deisseroth K. Simultaneous fast measurement of circuit dynamics at multiple sites across the mammalian brain. Nat Methods. 2016 Apr;13(4):325-8. doi: 10.1038/nmeth.3770. Epub 2016 Feb 15.

Kim U, Lee T (2012) Topography of descending projections from anterior insular and medial prefrontal regions to the lateral habenula of the epithalamus in the rat. *European Journal of Neuroscience* 35(8):1253–1269.

Kim U, Lee T (2012) Topography of descending projections from anterior insular and medial

prefrontal regions to the lateral habenula of the epithalamus in the rat. *Eur J Neurosci* 35(8):1253–1269.

Knowland D, Lilascharoen V, Pacia CP, Shin S, Wang EH, Lim BK. Distinct Ventral Pallidal Neural Populations Mediate Separate Symptoms of Depression. Cell. 2017 Jul 13;170(2):284-297.e18. doi: 10.1016/j.cell.2017.06.015. Epub 2017 Jul 6.

Kopec CD, Kessels HW, Bush DE, Cain CK, LeDoux JE, Malinow R. A robust automated method to analyze rodent motion during fear conditioning. Neuropharmacology. 2007 Jan;52(1):228-33. Epub 2006 Aug 22.

Lawson RP, Nord CL, Seymour B, Thomas DL, Dayan P, Pilling S, Roiser JP. Disrupted habenula function in major depression. Mol Psychiatry. 2017Feb;22(2):202-208. doi: 10.1038/mp.2016.81. Epub 2016 May 31.

Lecca S, Pelosi A, Tchenio A, Moutkine I, Lujan R, Hervé D, Mameli M. Rescue of GABAB and GIRK function in the lateral habenula by protein phosphatase 2A inhibition ameliorates depression-like phenotypes in mice. Nat Med. 2016 Mar;22(3):254-61. doi: 10.1038/nm.4037.

Lecca S, Meye FJ, Mameli M (2014) The lateral habenula in addiction and depression: an anatomical, synaptic and behavioral overview. *Eur J Neurosci* 39(7):1170–1178.

Li B, Piriz J, Mirrione M, Chung C, Proulx CD, Schulz D, Henn F, Malinow R. Synaptic potentiation onto habenula neurons in the learned helplessness model of depression. Nature. 2011 Feb 24;470(7335):535-9. doi: 10.1038/nature09742.

Li K, Zhou T, Liao L, Yang Z, Wong C, Henn F, Malinow R, Yates JR 3rd, Hu H. βCaMKII in lateral habenula mediates core symptoms of depression. Science. 2013 Aug 30;341(6149):1016-20. doi: 10.1126/science.1240729.

Lin JY, Lin MZ, Steinbach P, Tsien RY (2009) Characterization of Engineered Channelrhodopsin Variants with Improved Properties and Kinetics. *Biophysical Journal* 96(5):1803–1814.

Mahn M, Prigge M, Ron S, Levy R, Yizhar O (2016) Biophysical constraints of optogenetic inhibition at presynaptic terminals. *Nat Neurosci*. doi:10.1038/nn.4266.

Mattis J, Tye KM, Ferenczi EA, Ramakrishnan C, O'Shea DJ, Prakash R, Gunaydin LA, Hyun M, Fenno LE, Gradinaru V, Yizhar O, Deisseroth K. Principles for applying optogenetic tools derived from direct comparative analysis of microbial opsins. Nat Methods. 2011 Dec 18;9(2):159-72. doi: 10.1038/nmeth.1808.

Mill J, Petronis A (2007) Molecular studies of major depressive disorder: the epigenetic

perspective. *Mol Psychiatry* 12(9):799–814.

Morris JS, Smith KA, Cowen PJ, Friston KJ, Dolan RJ (1999) Covariation of activity in habenula and dorsal raphé nuclei following tryptophan depletion. *Neuroimage* 10(2):163–172.

Nabavi S, Fox R, Proulx CD, Lin JY, Tsien RY, Malinow R. Engineering a memory with LTD and LTP. Nature. 2014 Jul 17;511(7509):348-52. doi: 10.1038/nature13294. Epub 2014 Jun 1.

Nestler EJ, Carlezon WA (2006) The mesolimbic dopamine reward circuit in depression. *Biol Psychiatry* 59(12):1151–1159.

Parker KJ, Schatzberg AF, Lyons DM (2003) Neuroendocrine aspects of hypercortisolism in major depression. *Horm Behav* 43(1):60–66.

Pittenger C, Duman RS (2007) Stress, Depression, and Neuroplasticity: A Convergence of Mechanisms. *Neuropsychopharmacology* 33(1):88–109.

PORSOLT RD, Le Pichon M, JALFRE M (1977) Depression: a new animal model sensitive to antidepressant treatments. *Nature* 266(5604):730–732.

Proulx CD, Hikosaka O, Malinow R (2014) Reward processing by the lateral habenula in normal and depressive behaviors. *Nat Neurosci* 17(9):1146–1152.

Ranft K, Dobrowolny H, Krell D, Bielau H, Bogerts B, Bernstein HG. Evidence for structural abnormalities of the human habenular complex in affective disorders but not in schizophrenia. Psychol Med. 2010 Apr;40(4):557-67. doi: 10.1017/S0033291709990821. Epub 2009 Aug 12.

Roth KA, Katz RJ (1979) Stress, Behavioral Arousal, and Open Field Activity A Reexamination of Emotionality in the Rat. *Neuroscience & Biobehavioral Reviews* 3:247–263.

Rygula R, Abumaria N, Flügge G, Fuchs E, Rüther E, Havemann-Reinecke U. Anhedonia and motivational deficits in rats: impact of chronic social stress. Behav Brain Res. 2005 Jul 1;162(1):127-34. Epub 2005 Apr 14.

Sahay A, Hen R (2007) Adult hippocampal neurogenesis in depression. *Nat Neurosci* 10(9):1110–1115.

Salamone JD, Correa M (2012) The mysterious motivational functions of mesolimbic dopamine. *Neuron* 76(3):470–485.

Salamone JD, Koychev I, Correa M, McGuire P (2014) Neurobiological basis of motivational deficits in psychopathology. *European Neuropsychopharmacology*:1–14.

Sartorius A, Kiening KL, Kirsch P, von Gall CC, Haberkorn U, Unterberg AW, Henn FA, Meyer-

Lindenberg A. Remission of major depression under deep brain stimulation of the lateral habenula in a therapy-refractory patient. Biol Psychiatry. 2010 Jan 15;67(2):e9-e11. doi: 10.1016/j.biopsych.2009.08.027.

Shabel SJ, Proulx CD, Piriz J, Malinow R (2014) GABA/glutamate co-release controls habenula output and is modified by antidepressant treatment. *Science* 345(6203):1494–1498.

Shabel SJ, Proulx CD, Trias A, Murphy RT, Malinow R (2012) Input to the lateral habenula from the Basal Ganglia is excitatory, aversive, and suppressed by serotonin. *Neuron* 74(3):475–481.

Shumake J, Gonzalez-Lima F (2003) Brain systems underlying susceptibility to helplessness and depression. *Behav Cogn Neurosci Rev* 2(3):198–221.

Stamatakis AM, Van Swieten M, Basiri ML, Blair GA, Kantak P, Stuber GD. Lateral Hypothalamic Area Glutamatergic Neurons and Their Projections to the Lateral Habenula Regulate Feeding and Reward. J Neurosci. 2016 Jan 13;36(2):302-11. doi: 10.1523/JNEUROSCI.1202-15.2016.

Stamatakis AM, Stuber GD (2012) Activation of lateral habenula inputs to the ventral midbrain promotes behavioral avoidance. *Nat Neurosci*. doi:10.1038/nn.3145.

Tian L, Hires SA, Mao T, Huber D, Chiappe ME, Chalasani SH, Petreanu L, Akerboom J, McKinney SA, Schreiter ER, Bargmann CI, Jayaraman V, Svoboda K, Looger LL. Imaging neural activity in worms, flies and mice with improved GCaMP calcium indicators. Nat Methods. 2009 Dec;6(12):875-81. doi: 10.1038/nmeth.1398.

Treadway MT, Buckholtz JW, Cowan RL, Woodward ND, Li R, Ansari MS, Baldwin RM, Schwartzman AN, Kessler RM, Zald DH. Dopaminergic mechanisms of individual differences in human effort-based decision-making. J Neurosci. 2012 May 2;32(18):6170-6. doi: 10.1523/JNEUROSCI.6459-11.2012.

Treadway MT, Zald DH (2011) Reconsidering anhedonia in depression: Lessons from translational neuroscience. *Neuroscience & Biobehavioral Reviews* 35(3):537–555.

Tye KM, Mirzabekov JJ, Warden MR, Ferenczi EA, Tsai HC, Finkelstein J, Kim SY, Adhikari A, Thompson KR, Andalman AS, Gunaydin LA, Witten IB, Deisseroth K. Dopamine neurons modulate neural encoding and expression of depression-related behaviour. Nature. 2013 Jan 24;493(7433):537-541. doi: 10.1038/nature11740.

Vento PJ, Burnham NW, Rowley CS, Jhou TC (2017) Learning From One?s Mistakes: A Dual Role for the Rostromedial Tegmental Nucleus in the Encoding and Expression of Punished Reward Seeking. *Biol Psychiatry* 81(12):1041–1049.

Vollmayr B, Bachteler D, Vengeliene V, Gass P, Spanagel R, Henn F. Rats with congenital learned helplessness respond less to sucrose but show no deficits in activity or learning.

Behav Brain Res. 2004 Apr 2;150(1-2):217-21.

Warden MR, Selimbeyoglu A, Mirzabekov JJ, Lo M, Thompson KR, Kim SY, Adhikari A, Tye KM, Frank LM, Deisseroth K. A prefrontal cortex-brainstem neuronal projection that controls response to behavioural challenge. Nature. 2012 Dec 20;492(7429):428-32. doi: 10.1038/nature11617.

Yang L-M, Hu B, Xia Y-H, Zhang B-L, Zhao H (2008) Lateral habenula lesions improve the behavioral response in depressed rats via increasing the serotonin level in dorsal raphe nucleus. *Behavioural Brain Research* 188(1):84–90.

CHAPTER 2: Individual Vesicular Events Activating GABA and AMPA Receptors onto Lateral Habenula Neurons

Abstract

Co-release of neurotransmitters has been detected in numerous brain regions under physiological and pathological conditions. However, if the opponent neurotransmitters γ-aminobutyric acid (GABA) and glutamate are normally released from single vesicles is not well established. A recent exhaustive study demonstrated that GABA and glutamate are released from individual presynaptic neurons originating at several nuclei targeting the lateral habenula (LHb). Their anatomical techniques indicated that GABA-containing and glutamate containing presynaptic vesicles are segregated. Here we use electrophysiology to characterize a different synaptic projection onto the lateral habenula, and find that the majority of individual quantal events contain a dual glutamate and GABA composition. The lateral habenula may therefore have multiple means to balance excitation and inhibition by co-released GABA and glutamate.

Introduction

Evidence is mounting that challenges the textbook precept that a given neuron releases a single neurotransmitter (Hnasko and Edwards, 2012). With examples ranging from adenosine triphosphate (ATP) and acetylcholine (Ach) in electric rays (Whittaker et al., 1972; for review see: Burnstock, 2004), to GABA and glycine in neonatal rats (Bischofberger and Sandkuhler, 1998), to various permutations of glutamate, serotonin, and dopamine in cultured neurons (Johnson, 1994; Sulzer et al., 1998) and adult rodents (Nishimaru et al., 2005).

In some of these cases, the two neurotransmitters released by individual vesicles are “congruent,” as in the case of GABA and glycine, both of which canonically bind to receptors that result in the hyperpolarization of the post-synaptic cell. In other cases, such as with

glutamate and dopamine, the post-synaptic effects occur at different time-scales with a fast AMPA-receptor mediated component and a slow dopaminergic component.

Recent evidence suggests a pairing of transmitters that breaks the mold: The co-release of two fast-acting opponent neurotransmitters, GABA and glutamate (Shabel et al., 2014; Root et al., 2014). Moreover, electrophysiological and histological data suggests this is mediated, at least partially, by the release of vesicles with a dual GABAergic and glutamatergic composition (Shabel et al., 2014). A recent study demonstrated that a single neuron can release the two neurotransmitters, but their anatomical techniques indicate the two neurotransmitters are segregated to separate vesicles which can be present at the same axon terminal (Root et al., 2018). Here, we describe an electrophysiological and computational method for the identification of single-vesicle co-release of GABA and glutamate, and demonstrate that the majority of quantal events, at the LHA to LHb pathway, contain opponent neurotransmitters.

Results

Antero- and Retrograde Tracing Demonstrates Dense Projection from LHA to LHb

To test if the LHA provides an input to the LHb, we injected the retrograde tracer, subunit B of the cholera toxin, into the LHb of an adult rat (Figure A1) and observed a dense cluster of neurons in the anterior hypothalamic region (AP: -1.9), in concordance with previous studies (Stamatakis et al., 2016).

Next, to examine the projection pattern from LHA to LHb, we injected an anterograde virus expressing the fluorescent protein, tdTomato, into the LHA. We observed that axons from the LHA project to the medial aspect of the lateral habenula (Figure B3) almost entirely excluding the medial habenula and the lateral portion of the lateral habenula (which is more densely innervated by the entopeduncular nucleus (Shabel et al., 2014) and sends projections to the rostral medial tegmental nucleus (RMTg; Proulx, Aronson, et al., 2018)).

Taken in combination, these results indicate the presence a robust neuronal projection from the LHA to the LHb.

Mixed Excitatory and Inhibitory Transmission from the LHA to the LHb

To examine synaptic transmission between the LHA and LHb, animals were injected, as before, with an AAV expressing OChIEF in the LHA. 2-3 weeks later, acute slices were made for electrophysiology. We observed evidence of inward and outward currents upon optical stimulation at various holding potentials (Figure 2A1, -60, -45, -35, -15, 0, +15 mV). At a holding potential of -35 mV, biphasic currents were observed (Figure 2A2). Average ratio of inward to outward current, measured at -42mV and 0mV respectively, was 2.1 +/- .3 (animal_n = 6; slice_n = 8; cell_n = 14).

To examine the nature of the quantal events that compose these evoked post-synaptic currents, the bathing solution had $CaCl_2$ replaced with $SrCl_2$. Under such conditions synchronous transmitter release is reduced and asynchronous quantal release is greatly enhanced (Miledi et al., 1966; Meiri and Rahamimoff, 1971; Zengel and Magleby, 1980; Bain and Quastel, 1992; Goda and Stevens, 1994). The internal solution of the recording electrode was also modified with a high chloride solution so that the opening of GABA-activated chloride channels produced inward currents at hyperpolarized potentials (see methods). Under these conditions, optically evoked miniature post synaptic currents (minis; Figure 2B1) were readily observed. We reasoned that since the currents produced by AMPA-Rs and GABA-A-Rs have different kinetics, individual quanta opening only AMPA-Rs, only GABA-A-Rs, or both, may be distinguishable. Examples of minis evoked in the presence of gabazine (2B2) and NBQX (2B3) are shown in Figure 2B. The frequency of evoked minis fell to 0 when both gabazine and NBQX were applied (cell_n = 3, animal_n = 3), suggesting these minis are comprised exclusively of AMPA-R and GABA-A-R currents.

Clear Separation of Excitatory and Inhibitory Quantal Events

Datasets of pharmacologically isolated excitatory minis or inhibitory minis were obtained by the use of GABAzine (to block GABA-A-Rs; animal_n = 4, slice_n = 4, cell_n = 13, mini_n = 100) and NBQX (to block AMPARs; animal_n = 3, slice_n = 3, cell_n = 5, mini_n = 100). For each dataset, minis were identified and the following measures were obtained (see methods): amplitude, rise time, decay time, area under the curve, half width, time from 10% to 90% of rise, and time from 10% to 90% of decay. A compiled dataset was created with equal numbers of excitatory and inhibitory minis. We applied a principal component analysis (PCA) on the measures of events for the compiled dataset. Briefly, PCA is a statistical procedure that uses an orthogonal transformation to convert a set of variables, in this case descriptive statistics of individual minis, into linearly uncorrelated variables called principal components. The first component (PC1) explains the most variance within the dataset, followed by the second (PC2), etcetera. In this case, we are using PCA as an unbiased approach to maximize variable across minis without previous knowledge of their identity (excitatory or inhibitory). Plotting each event on two or three principal components (Figure 3A) revealed a clear qualitative separation of the excitatory (blue) and inhibitory (green) minis (variance explained by PC: PC 1 (72%); PC 2 (16%), PC 3 (6%)). The variables that contributed the most to each PC were: 10-90 slope (.93 of PC 1); Decay time (.70 of PC 2); Amplitude (.76 of PC 3).

Third Population of Quantal Events Not Fully Explained by Excitatory or Inhibitory Measures

Next a dataset of evoked minis was acquired in the absence of blocking agents (animal_n = 3; slice_n = 3; cell_n = 3; mini_n = 100). These were identified and quantified, as above, and projected into the PC space that was generated with the counter-balanced, pharmacologically “pure” groups. Clear evidence of a third group of quantal events emerges as these minis (pink) can not be entirely explained by the two other groups.

Dual Component Quantal Event Appears to be Linear Sum of Single-Component Events

Average waveforms reveal excitatory minis have a faster rise and faster decay than their inhibitory counterparts (Figure 2.4A). Minis recorded in absence of blocking agents (animal_n = 3; slice_n = 3; cell_n = 3; mini_n = 100) have an intermediate rise and decay and appear to be a linear sum of the two components (pink trace, Figure 2.4A).

Linear Model Can Predict Composition of Quantal Event

To test whether we could predict the excitatory to inhibitory ratio of individual quantal events, a synthetic dataset was generated by linearly combining a known fraction of the mean excitatory trace with a known fraction of the mean inhibitory trace (Figure 2.3B, light→darker::more excitatory→more inhibitory; Uniform distribution).

We next performed PCA on the waveform segments themselves, aligned to the onset of the event and lasting 500ms. Coefficients were generated, as before, only using isolated excitatory and inhibitory events. We observe similar separation of observed (pink circles, 2.4C) and synthetic (pink circles, 2.4D) minis in PC space. Interestingly, a ratio of PC1/PC3 readily predicted ground truth of the synthetic dataset (2.4E) and a linear model could be used to accurately predict ground truth from these two components (2.4F; R^2 = .91, $p < .0001$; predicted_fraction_AMPA = .85(PC1/PC3) + .9). To account for some uncertainty when a mini is predominantly excitatory or predominantly inhibitory, a cutoff was applied such that if predicted_fraction_AMPA > .9 → = 1 and if predicted_fraction_AMPA < .9 → = 1.

Applying this methodology to the pharmacologically isolated group, we can observe clear separation of the two groups (2.4F; unpaired t-test, $p < .0001$; excitatory = .81 +/- .001; inhibitory = .25 +/- .002). The observed minis form a distinct population (2.4H) that is separate from the purely excitatory ($p < .00001$) and purely inhibitory ($p < .00001$) groups (corrected for multiple tests). The observed population is consistent with quantal events that are an equal

mixture of the response activated by pure GABA and pure AMPA minis, with a Gaussian distribution centered at .55 %AMPA (sigma = .23).

Methods:

Surgery

Male Sprague-Dawley rats, age 28-32 days at time of surgery (42-46 days when sacrificed for slice experiments), were housed 1-4/cage and kept on a 12/12 hour light-dark cycle (lights on/off at 6 am/6 pm). Rats were anesthetized with isoflurane for stereotaxic bilateral injection of AAV virus into the LHA (AP: -1.9 mm from bregma; ML: 1.7 mm from midline; DV: -7.5 mm from top of skull) or the retrograde tracer into the LHb (AP: -3.4 mm from bregma; ML: .6 mm from midline; DV: -4.8 mm from top of skull). ~500 nl of virus or Ctx was wer injected into each hemisphere over 8-20 minutes using a picospritzer. Rats were injected subcutaneously with 5 mg/kg carprofen (NSAID) after surgery.

Virus Preparation

The cDNA encoding DIO and non-DIO version of the oChiEf variant of ChR2 was a gift from the lab of Dr. Roger Tsien. Virus was prepared as before (Shabel et al., 2014) and titers ranged from $1x10^{11}$ GC to $1x10^{12}$ GC.

Electrophysiology

Two weeks after injection, rats were anesthetized with isoflurane before rapid decapitation and extraction of the brain. Brains were chilled in ice-cold dissection buffer (110.0 mM choline chloride, 25.0 mM $NaHCO_3$, 1.25 mM NaH_2PO_4, 2.5 mM KCl, 0.5 mM $CaCl_2$, 7.0 mM $MgCl_2$, 25.0 mM glucose, 11.6 mM ascorbic acid, 3.1 mM pyruvic acid; gassed with 95%O_2/5%CO_2) and cut in 400 micron thick coronal slices through the LHb. Slices were

transferred to 35 oC ACSF (118 mM NaCl, 2.5 mM KCl, 26.2 mM $NaHCO_3$, 1 mM NaH_2PO_4, 20 mM Glucose, 1 mM $MgCl_2$, 2 mM $CaCl_2$; 22°–25°C; pH 7.4; gassed with 95%O_2/5%CO_2) for 30 minutes. After an additional 30 minutes of recovery at room temperature, slices were transferred to the recording chamber and constantly perfused with room temperature (22°–25°C) ACSF. Remaining tissue, containing the LHA, was fixed in 4% paraformaldehyde solution overnight before being mounted on slides to confirm injection site.

Recordings were made from cells in the medial aspect of the LHb, where LHA inputs were densest as confirmed by epifluorescent imaging, using an Axopatch 1D amplifier with a 1-5kHz sampling frequency and a filter set at a -3dB cutoff frequency of 5kHz. For voltage-clamp recordings the intracellular solution consisted of (in mM): 7.5 QX314, 115 cesium methanesulfonate, 20 CsCl, 10 HEPES, 2.5 $MgCl_2$, 4 Na_2-ATP, 0.4 Na-GTP, 10 Na-phosphocreatine, and 0.6 EGTA (pH 7.2). 470 nm light was delivered via a mercury arc lamp and excitation filter (458-40 nm) and delivered to the slice through the objective. To observe light-evoked post-synaptic currents are various holding potentials, a single 5ms pulse was delivered. All recordings took place in the presence of D-APV (100 μM). E:I ratio was calculated as the average of 10 evoked current at -42 mV (reversal potential for GABA) or 0 mV (reversal potential for AMPA).

To examine optically evoked asynchronous quantal events, slices were transitioned from the recovery chamber to a strontium-based ACSF solution on the rig (118 mM NaCl, 2.5 mM KCl, 26.2 mM $NaHCO_3$, 1 mM NaH_2PO_4, 20 mM Glucose, 1 mM $MgCl_2$, 2 mM $StCl_2$; 22°–25°C; pH 7.4; gassed with 95%O_2/5%CO_2) and cells were patched with a high chloride internal solution (7.5 mM QX314, 115 mM cesium methanesulfonate, 100 mM CsCl, 10 mM HEPES, 2.5 mM MgCl2, 4 mM Na2-ATP, 0.4 mM Na-GTP, 10 mM Na- phosphocreatine, and 0.6 EGTA mM (pH 7.2)). Stimulation was titrated to produce isolatable miniature post synaptic currents (from a

single 5ms light pulse to 5 x 5 ms light pulses at 20 hz). All recordings took place in the presence of D-APV (100 μM). Recordings to isolate AMPA-mediated minis occurred in the presence of GABAzine (100 uM). Recordings to isolate AMPA-mediated minis occurred in the presence of NBQX (3 uM).

Analysis

Miniature post-synaptic currents were identified and quantified using Minianalysis software. All computational analyses were performed in MATLAB (Mathworks 2014). Principal component analysis was performed using the embedded function ([coeff] = pca) on a matrix containing equal numbers of excitatory (recorded in GABAzine; animal_n = 4, slice_n = 4, cell_n = 13, mini_n = 100) and NBQX (recorded in AMPARs; animal_n = 3, slice_n = 3, cell_n = 5, mini_n = 100). The matrix was organized as mini_n in rows and descriptive statistics in columns. Minis were projected into “PC space” by taking the product of the original matrix and the PC coefficients.

Subsequent analyses (Fig. 2.4B) utilized a synthetic dataset of mixed minis with known composition was generated by taking the sum of X*(mean_inhibitory) + (1-X)*(mean_excitatory) and adding white Gaussian noise (function = awgn). Amplitudes of these synthetic minis were randomly scaled to individual excitatory or inhibitory components.

Principal component analysis was performed, not on descriptions of the waveforms (as above), but on the waveforms themselves. As before, the coefficients were generated using only the isolated excitatory and inhibitory events. A linear fit of PC1/PC3 to the ground truth composition of the synthetic group (function = fitlm) allowed us to estimate the composition of an individual quantal event from its location in PC space. To account for uncertainty when a mini was predominantly excitatory or predominantly inhibitory, a non-linear cutoff was applied such that values > .9 → 1 and values < .1 → 0. Percentage AMPA (% AMPA) is always in reference to a GABAergic component – ie if % AMPA is high, % GABA is low, etc.

Discussion

We developed a technique to detect the presence of quantal events with both a GABAergic and glutamatergic component. We then demonstrated that many cells in a hypothalamic projection to the LHb contain these dual-component minis, indicative of single vesicle release of two opponent neurotransmitters.

Despite the dogma that GABA and glutamate are segregated to separate populations of neurons, evidence of single-neuron co-release is mounting in the LHb (Shabel et al., 2014; Root et al., 2014; Meye et al., 2016), dentate gyrus (Soussi et al., 2010; Pedersen et al., 2017), lateral superior olive (Gillespie et al., 2005; Noh et al., 2010), and cortex (Fattorini et al., 2015). Ultrastructural data suggests that, for some projections to the LHb, within a single axon terminal, neurotransmitters are segregated to independent vesicle pools that form symmetric (inhibitory) and asymmetric (excitatory) synapses (Root et al., 2018). Other habenular projections, such as those from the EP and the LHA release single vesicles with a dual-component (Shabel et al., 2014), suggesting the LHb may have multiple mechanisms of balancing excitation and inhibition.

Our findings give rise to a quandary: Why would a neuron release opponent neurotransmitters from single vesicles? At first pass, this seems energetically unfavorable as the AMPA-mediated current would be partially shunted by the GABA-mediated current. Some have argued this mechanism, and its dynamism in cases of addiction and disease models, could be important for the processing of reward prediction error (Uchida, 2014; Root et al., 2014; Shabel et al., 2014; Stamatakis and Stuber, 2012). There are two additional ways this could have biological utility. 1) The LHb is largely devoid of interneurons (Brinschwitz et al., 2010). Another mechanism may be required to prevent runaway excitation. As the time-course of AMPA-mediated currents is an order of magnitude faster than that of GABA-mediated currents, driving pre-synaptic firing results in a time-locked action potential followed by 100s of

ms long period of inhibition (Shabel et al., 2014). It stands to reason that as the presynaptic firing rate increases, the GABAergic currents will begin to summate before the AMPAergic currents, resulting in a non-linear input/output function where, at low frequencies, a tract is net excitatory and, at higher frequencies, it is net inhibitory. 2) The LHb is cell sparse, yet receives inputs from a wide array of brain regions (Proulx et al., 2014). This necessitates a certain degree of convergence. Co-release of GABA and glutamate could represent a mechanism by which inputs can compete to drive the post-synaptic cell to their preferred firing rate. As a presynaptic tract fires, it drives the post-synaptic neuron via AMPA-mediated current. In turn, the inhibitory current in the inter-spike interval decreases the likelihood that another tract could drive the target neuron to fire.

Further research is required to elucidate the utility of single-vesicle co-release of GABA and glutamate and its function in both physiological and pathological conditions.

Chapter 2, in full, is in preparation for publication. Aronson, SR, Malinow, RM. “Individual Vesicular Events Activating GABA and AMPA Receptors onto Lateral Habenula Neurons.” The dissertation author was the primary investigator and author of this publication.

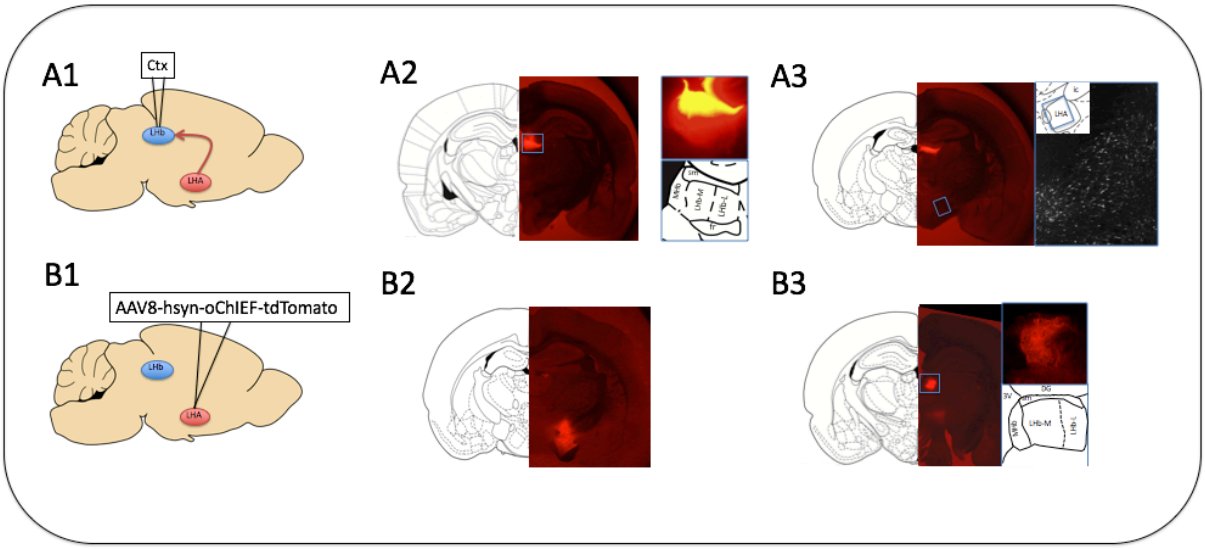

Figure 2.1. The LHA sends a dense axonal projection to the LHb. A1) Cartoon of experimental design for retrograde tracing. A2) Image of injection site localized in the *stria medularis*. A3) Epifluorescent (left) and confocal (right) images of LHA. B1) Cartoon of experimental design for anterograde tracing. B2) Image of injection site localized in dorsal aspect of the LHA. B3) Epifluorescent (left) and confocal (right) images of LHb. Axons from cells in the LHA preferentially project to the medial aspect of the LHb.

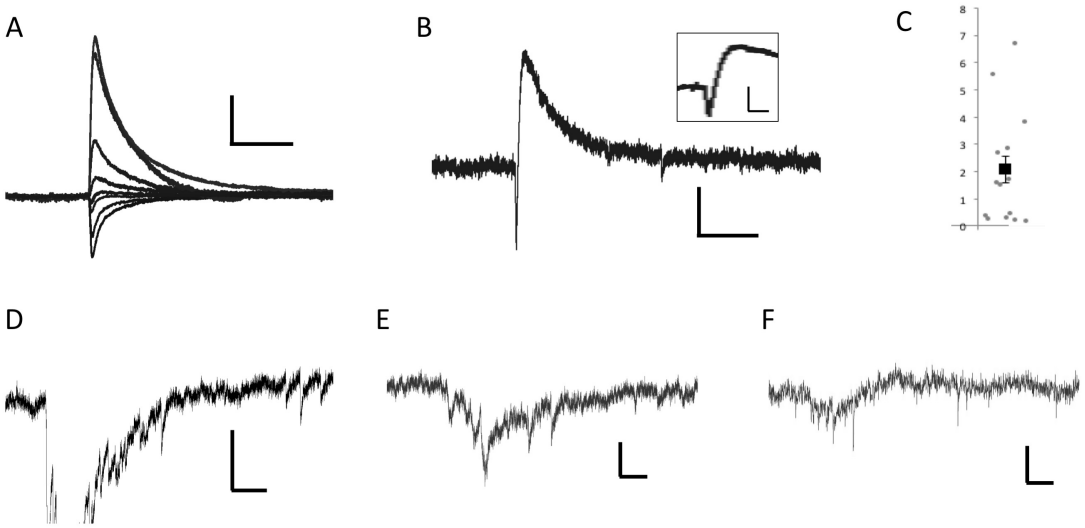

Figure 2.2. Synchronous and Asynchronous Release of GABA and glutamate onto LHb neurons. A) Optical stimulation of LHA axons results in both inward and outward currents. Whole-cell voltage clamp recordings of LHb neurons at currents at various holing potentials. From top to bottom (+15, +5, 0, -15, -25, -35, -42, -60 mV; scale bars: vertical = 100 pA, horizontal = 100 ms) B) Biphasic current, with fast inward and slow outward component observed at intermediate holding potential (inset is a scaled version of larger trace, holding potential: -35 mV; scale bars: 10pA, 100 ms for 2B and 2B inset). C) Ratio of Inward to Outward Current. 2.1 +/- .3. n_{cells} = 14. D) Optical stimulation with bath strontium replacing calcium results in asynchronous neurotransmitter release (scale bars: 20 pA, 1 second). E) Evoked minis in the presence of NBQX (scale bars: 10 pA, 1 second). F) Evoked minis in the presence of GABAzine (scale bars: 20 pA, 1 second).

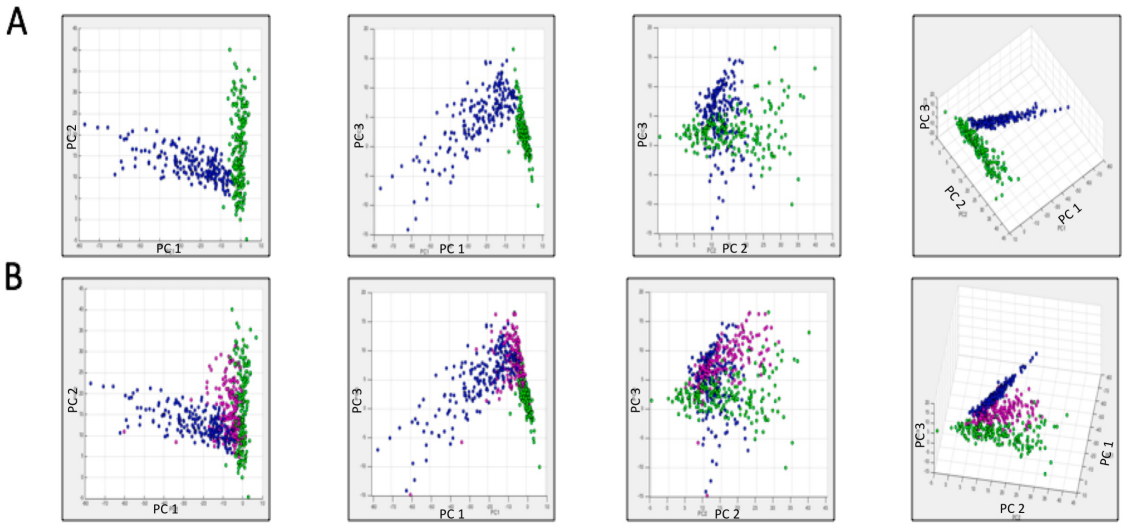

Figure 2.3: Principal Component Analysis Reveals Quantal Events Are Neither Purely GABAergic or purely glutamatergic. Blue = AMPA mediated minis. Green = GABAergic minis. Pink = minis observed in the absence of blocking agents. A) Clear separation of excitatory and inhibitory minis. PCs generated using only counterbalanced AMPA and GABA minis. B) Test minis comprise a separate population that is neither purely GABAergic or purely glutamatergic.

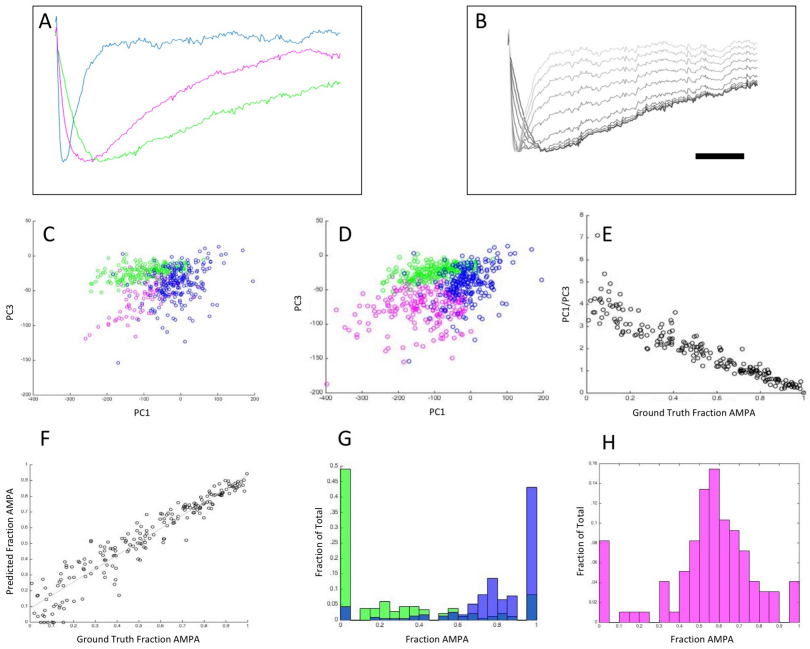

Figure 2.4: Linear model predicts excitatory/inhibitory components of individual quantal events. A) Average waveform of observed minis (pink) compared to average waveform of pharmacologically isolated AMPAergic (blue) and GABAergic minis (green). B) A synthetic dataset was generated with known values of AMPA to GABA. Light → Dark::AMPA →GABA. Scale bar = 100 ms, amplitude has been normalized (a.u.). Distribution of observed C) or synthetic minis D) in PC space. E) PC1/PC3 can predict ground truth ($p < .00001$; $r^2 = .91$). F) Using a linear model, we can predict %AMPA from PC1/PC3. G) Clear separation of AMPAergic (.81 +/- .001) and GABAergic (.25 +/- .002) minis by this metric ($p < .00001$). H) Observed population (.55 +/- .002) was significantly different than isolated AMPAergic ($p < .00001$) and GABAergic populations ($p < .00001$).

References

Bain AI, Quastel DM. Quantal transmitter release mediated by strontium at the mouse motor nerve terminal. J Physiol. 1992 May;450:63-87. PubMed PMID: 1359125; PubMed Central PMCID: PMC1176111.

Brinschwitz K, Dittgen A, Madai VI, Lommel R, Geisler S, Veh RW. Glutamatergic axons from the lateral habenula mainly terminate on GABAergic neurons of the ventral midbrain. Neuroscience. 2010 Jun 30;168(2):463-76. doi: 10.1016/j.neuroscience.2010.03.050. Epub 2010 Mar 29. PubMed PMID: 20353812.

Burnstock G. Cotransmission. Curr Opin Pharmacol. 2004 Feb;4(1):47-52. Review. PubMed PMID: 15018838.

Fattorini G, Antonucci F, Menna E, Matteoli M, Conti F. Co-expression of VGLUT1 and VGAT sustains glutamate and GABA co-release and is regulated by activity in cortical neurons. J Cell Sci. 2015 May 1;128(9):1669-73. doi: 10.1242/jcs.164210. Epub 2015 Mar 6. PubMed PMID: 25749864.

Goda Y, Stevens CF. Two components of transmitter release at a central synapse. Proc Natl Acad Sci U S A. 1994 Dec 20;91(26):12942-6. PubMed PMID: 7809151; PubMed Central PMCID: PMC45556.

Hnasko TS, Edwards RH. Neurotransmitter corelease: mechanism and physiological role. Annu Rev Physiol. 2012;74:225-43. doi: 10.1146/annurev-physiol-020911-153315. Epub 2011 Oct 31. Review. PubMed PMID: 22054239; PubMed Central PMCID: PMC4090038.

Johnson MD. Synaptic glutamate release by postnatal rat serotonergic neurons in microculture. Neuron. 1994 Feb;12(2):433-42. PubMed PMID: 7906530.

Jonas P, Bischofberger J, Sandkühler J. Corelease of two fast neurotransmitters at a central synapse. Science. 1998 Jul 17;281(5375):419-24. PubMed PMID: 9665886.

Meiri U, Rahamimoff R. Activation of transmitter release by strontium and calcium ions at the neuromuscular junction. J Physiol. 1971 Jul;215(3):709-26. PubMed PMID: 4326307; PubMed Central PMCID: PMC1331909.

Meye FJ, Soiza-Reilly M, Smit T, Diana MA, Schwarz MK, Mameli M. Shifted pallidal co-release of GABA and glutamate in habenula drives cocaine withdrawal and relapse. Nat Neurosci. 2016 Aug;19(8):1019-24. doi: 10.1038/nn.4334. Epub 2016 Jun 27. PubMed PMID: 27348214.

Miledi R. Strontium as a substitute for calcium in the process of transmitter release at the neuromuscular junction. Nature. 1966 Dec 10;212(5067):1233-4. PubMed PMID: 21090447.

Noh J, Seal RP, Garver JA, Edwards RH, Kandler K. Glutamate co-release at GABA/glycinergic synapses is crucial for the refinement of an inhibitory map. Nat Neurosci. 2010 Feb;13(2):232-8. doi: 10.1038/nn.2478. Epub 2010 Jan 17. PubMed PMID: 20081852; PubMed Central PMCID: PMC2832847.

Pedersen NP, Ferrari L, Venner A, Wang JL, Abbott SBG, Vujovic N, Arrigoni E, Saper CB, Fuller PM. Supramammillary glutamate neurons are a key node of the arousal system. Nat Commun. 2017 Nov 10;8(1):1405. doi: 10.1038/s41467-017-01004-6. PubMed PMID: 29123082; PubMed Central PMCID: PMC5680228.

Proulx CD, Aronson S, Milivojevic D, Molina C, Loi A, Monk B, Shabel SJ, Malinow R. A neural pathway controlling motivation to exert effort. Proc Natl Acad Sci U S A. 2018 May 29;115(22):5792-5797. doi: 10.1073/pnas.1801837115. Epub 2018 May 11. PubMed PMID: 29752382; PubMed Central PMCID: PMC5984527.

Root DH, Zhang S, Barker DJ, Miranda-Barrientos J, Liu B, Wang HL, Morales M. Selective Brain Distribution and Distinctive Synaptic Architecture of Dual Glutamatergic-GABAergic Neurons. Cell Rep. 2018 Jun 19;23(12):3465-3479. doi: 10.1016/j.celrep.2018.05.063. PubMed PMID: 29924991.

Root DH, Mejias-Aponte CA, Zhang S, Wang HL, Hoffman AF, Lupica CR, Morales M. Single rodent mesohabenular axons release glutamate and GABA. Nat Neurosci. 2014 Nov;17(11):1543-51. doi: 10.1038/nn.3823. Epub 2014 Sep 21. PubMed PMID: 25242304; PubMed Central PMCID: PMC4843828.

Shabel SJ, Proulx CD, Piriz J, Malinow R. Mood regulation. GABA/glutamate co-release controls habenula output and is modified by antidepressant treatment. Science. 2014 Sep 19;345(6203):1494-8. doi: 10.1126/science.1250469. Epub 2014 Sep 18. PubMed PMID: 25237099; PubMed Central PMCID: PMC4305433.

Soussi R, Zhang N, Tahtakran S, Houser CR, Esclapez M. Heterogeneity of the supramammillary-hippocampal pathways: evidence for a unique GABAergic neurotransmitter phenotype and regional differences. Eur J Neurosci. 2010 Sep;32(5):771-85. doi: 10.1111/j.1460-9568.2010.07329.x. Epub 2010 Aug 16. PubMed PMID: 20722723; PubMed Central PMCID: PMC2974797.

Soussi R, Boulland JL, Bassot E, Bras H, Coulon P, Chaudhry FA, Storm-Mathisen J, Ferhat L, Esclapez M. Reorganization of supramammillary-hippocampal pathways in the rat pilocarpine model of temporal lobe epilepsy: evidence for axon terminal sprouting. Brain

Struct Funct. 2015 Jul;220(4):2449-68. doi: 10.1007/s00429-014-0800-2. Epub 2014 Jun 3. PubMed PMID: 24889162; PubMed Central PMCID: PMC4481331.

Stamatakis AM, Van Swieten M, Basiri ML, Blair GA, Kantak P, Stuber GD. Lateral Hypothalamic Area Glutamatergic Neurons and Their Projections to the Lateral Habenula Regulate Feeding and Reward. J Neurosci. 2016 Jan 13;36(2):302-11. doi: 10.1523/JNEUROSCI.1202-15.2016. PubMed PMID: 26758824; PubMed Central PMCID: PMC4710762.

Sulzer D, Joyce MP, Lin L, Geldwert D, Haber SN, Hattori T, Rayport S. Dopamine neurons make glutamatergic synapses in vitro. J Neurosci. 1998 Jun 15;18(12):4588-602. PubMed PMID: 9614234.

Whittaker VP, Dowdall MJ, Boyne AF. The storage and release of acetylcholine by cholinergic nerve terminals: recent results with non-mammalian preparations. Biochem Soc Symp. 1972;(36):49-68. Review. PubMed PMID: 4374951.

Zengel JE, Magleby KL. Differential effects of Ba2+, Sr2+, and Ca2+ on stimulation-induced changes in transmitter release at the frog neuromuscular junction. J Gen Physiol. 1980 Aug;76(2):175-211. PubMed PMID: 6967950; PubMed Central PMCID: PMC2228595.